Ocean Engineering 291 (2024) 116464

Contents lists available at ScienceDirect

Ocean Engineering

journal homepage: www.elsevier.com/locate/oceaneng

Air quality forecasting of along-route ship emissions in realistic meteo-marine scenarios

Andrea Orlandi [a], Francesca Calastrini [b], Miltiadis Kalikatzarakis [c], Francesca Guarnieri [a], Caterina Busillo [a], Andrea Coraddu [d,*]

[a] Consorzio LaMMA, Florence, Italy
[b] CNR-IBIMET, Florence, Italy
[c] University of Strathclyde, Glasgow, United Kingdom
[d] Faculty of Mechanical, Maritime and Materials Engineering, Delft University of Technology, Delft, The Netherlands

ARTICLE INFO

Keywords:
Ship emissions
Seakeeping
Ship performance modeling
Air quality modeling

ABSTRACT

This study introduces a novel framework of metocean prediction and ship performance models that integrate multiple layers of modeling to evaluate the environmental impact of ship emissions. It enables scenario simulations that assess a ship's performance, estimates pollutant emissions, and simulate the fate of these pollutants in the atmosphere. The study analyzes the fate of NOx, SO_2, and PM10 pollutants in the atmosphere using spatially distributed concentration maps. It provides a comprehensive approach to assessing the environmental effects of ships and their emissions and contributes to the field of environmental impact assessment. Case studies are presented to demonstrate the framework's functionalities, evaluating the interrelationships between adverse meteo-marine conditions, pollutant emissions, and resulting atmospheric diffusion characteristics.

1. Introduction

International shipping accounts for approximately 80% of the global trade by value (Asariotis et al., 2019), and has always been the fuel- and cost-efficient mode of transport (Gabrielli and von Karman, 1950; Trancossi, 2016; Bejan et al., 2019). Currently, ship-related emissions are the center stage of the world shipping community (van Aardenne et al., 2013), with increasing regulatory pressure to achieve greener maritime transportation, control gaseous emissions, and air pollution, and reduce the environmental impact of the maritime industry.

1.1. Regulatory framework

Various international and national regulatory bodies such as International Maritime Organisation (IMO), European Maritime Safety Agency (EMSA) and the United States Environmental Protection Agency (EPA) have adopted a series of regulations for limiting non-greenhouse gaseous emissions, including NO_x and SO_x, as well as the greenhouse gaseous emissions, with the main concern being CO_2 (Smith et al., 2014; Buhaug et al., 2009). Despite these efforts, maritime transport emits around 940 million tonnes of CO_2 annually. It is responsible for about 2.5% of global greenhouse gas emissions (Smith et al., 2014) with the potential to increase between 50% and 25% by 2050, undermining the objectives of the Paris Agreement (Agreement, 2015). The shipping industry responded with the adoption of energy efficiency and emissions reduction measures, both at the design (Energy Efficiency Design Index — EEDI) and the operational stages (Energy Efficiency Management Plan - SEEMP) (IMO, 2011). Furthermore, to keep pace with the evolving landscape of emissions regulation and reduction, more recent mechanisms such as the CII (Carbon Intensity Indicator) and the EEXI (Energy Efficiency Existing Ship Index) have been developed (Baldi and Coraddu, 2022). The CII is an innovative approach that measures the carbon intensity of a ship's operations. It acts as a performance-based metric, tracking the CO_2 emissions of a vessel relative to its transport work. With this mechanism, shipowners and operators can continuously monitor and optimize their fleet's environmental performance, focusing not just on the design of new vessels but also on the operational efficiency of existing ones. By having a standardized metric, the shipping industry can better benchmark and drive improvements in reducing carbon intensity. While the EEDI focused on new ship designs, there was a recognized gap in addressing the vast fleet of existing ships. The EEXI fills this void. It mandates a set of energy efficiency requirements for existing ships, ensuring

* Corresponding author.
E-mail addresses: orlandi@lamma.rete.toscana.it (A. Orlandi), calastrini@lamma.rete.toscana.it (F. Calastrini), miltiadis.kalikatzarakis@strath.ac.uk (M. Kalikatzarakis), guarnieri@lamma.rete.toscana.it (F. Guarnieri), busillo@lamma.rete.toscana.it (C. Busillo), a.coraddu@tudelft.nl (A. Coraddu).

https://doi.org/10.1016/j.oceaneng.2023.116464
Received 8 June 2023; Received in revised form 23 November 2023; Accepted 27 November 2023
Available online 3 December 2023
0029-8018/© 2023 The Author(s). Published by Elsevier Ltd. This is an open access article under the CC BY license (http://creativecommons.org/licenses/by/4.0/).

that they meet specific standards in terms of their operational carbon intensity. The aim is to retrofit and upgrade older ships to ensure they are more fuel-efficient, thereby reducing their overall greenhouse gas emissions. This initiative is particularly vital as it targets the bulk of the global fleet, ensuring that older ships are not left behind in the industry's push for sustainability. Simultaneously, the IMO's Marine Environment Protection Committee (MEPC), during its 80th session, unveiled new carbon targets, reflecting a heightened commitment to curbing greenhouse gas emissions from shipping. These targets not only set stricter limits on carbon emissions but also provide a roadmap for the gradual decarbonization of the industry, aiming for a considerable reduction by 2050. The MEPC's proactive stance reaffirms the global intent to align maritime operations with international climate goals, most notably the objectives set out in the Paris Agreement. These recent mechanisms and targets serve as testamentary evidence of the shipping industry's evolving commitment to sustainability, highlighting a concerted effort to minimize its environmental impact while meeting the ever-increasing global trade demands.

For a sound decision-making process, both at the operational and legislative levels, detailed knowledge of the environmental conditions and their mutual interrelations with shipping activities is required. Therefore, environmental modeling approaches are highly relevant, especially when implemented in a multidisciplinary framework (Huszar et al., 2010; Tang et al., 2020).

1.2. Modeling approaches for emission inventories

A relevant topic where multidisciplinary simulations are involved is related to the construction of emission inventories. These are produced by merging data regarding the shipping traffic in a given area with technical data regarding the propulsion systems and the corresponding emissions for all the relevant ships involved, and in some cases, data regarding environmental metocean conditions. A combination of statistical processing (to correctly account for the various features of the ship's population in the area) and physical modeling approaches is usually adopted (Nunes et al., 2017). In this framework, emission inventories have been produced with different detail levels and data layers included. An in-depth discussion and systematic comparison of the various emission inventories are reported in van Aardenne et al. (2013). Some of the differences are related to geographical modeling elements, and others come from unequal ship traffic populations or from taking into account diverse regulations of ship traffic or, e.g., fuel sulfur content (Jalkanen et al., 2016). Other differences are related the details of ship modeling approaches and the presence/absence of environmental effects. Moreover, the very simplified treatment of the latter can be the source of some degree of uncertainty (Segersson, 2013), and as a result, discrepancies among the inventories are reported in the literature (Jalkanen et al., 2016). It must be admitted that some of the simplifications in the modeling detail of ship performance and environmental effects on them are needed to limit the computational effort when a wide population of ships and long time periods are considered when generating comprehensive inventories.

Multi-fidelity modeling approaches have been extensively adopted for shipping emissions inventories. For instance, the *Air pollutant emission inventory guidebook* of the European Environmental Agency's European Monitoring and Evaluation Programme (Trozzi and De Lauretis, 2019), or the *inventories of shipping emissions* in China (Fu et al., 2017). The purpose of these modeling approaches is twofold: they are necessary for the compilation of these inventories, as well as for the conduct of environmental impact studies. The compilation of emissions inventories requires gathering technical and operational data for various ship types operating in the area under consideration. In some relevant studies, this data is extracted from the Automatic Identification System and combined with multi-fidelity modeling approaches. Relevant examples are the works of the Finnish Meteorological Institute (FMI), conducted initially for the Baltic Sea (Jalkanen et al., 2009) and then extended to most of the European sea areas (Jalkanen et al., 2016), and the works of the Swedish Meteorological and Hydrological Institute, for the Baltic Sea (Segersson, 2013). In particular, the Ship Traffic Emission Assessment Model (STEAM) developed by FMI (Jalkanen et al., 2009, 2016) is one of the most detailed and widely used models (Corbett et al., 2016; Zhang et al., 2017; Majamäki et al., 2021).

The most common approach in these studies is to consider the total emissions as the sum of each vessel's emissions operating in the investigated area. The latter is assessed by using average data from broad ship type classes (Jalkanen et al., 2016) due to the high number of vessels operating at the same time. Whereas this approach allows for a numerically inexpensive assessment of a complex scenario, several key elements can be inaccurate. For instance, the dependence of emissions on the engine type, fuel type, and sailing mode (i.e., cruising, manoeuvring) is difficult to capture (Trozzi, 2010). Moreover, the dependence of emissions on engine load, and hence on the encountered meteo-marine conditions are also frequently neglected. An exception is the STEAM model (Jalkanen et al., 2016), which accounts for meteo-marine conditions considering the effect of the added resistance in waves to the engine load. In particular, the model applies a speed penalty (Jalkanen et al., 2009; Townsin et al., 1993) that has a very simplified dependence on the main particulars of the vessel (e.g., ship type and displacement) and that is related to the metocean conditions only through the Beaufort number. Also, winds and marine currents could be accounted for, but these are considered less relevant because a sort of cancellation is expected due to mutual cancellations of the favorable and unfavorable conditions in averaging over long time periods (Jalkanen et al., 2016). However, further studies should be performed to systematically and precisely evaluate the real relevance of the different environmental factors on the overall emission pattern in a given area, also considering possible evolution trends due to climate change.

1.3. Detailed modeling approaches

Approaches based on detailed modeling of ship performance in relation to environmental conditions have been developed both in the context of ship design and ship trials data processing (Lewis, 1988; Bertram, 2011; Vossen et al., 2013; Papanikolaou, 2019; Calleya et al., 2015; van den Boom et al., 2006; International Standards Organization, 2015) and in the context of weather routing and operational guidance systems (Pacheco and Guedes Soares, 2007; Simonsen et al., 2015; Lu et al., 2015; Yoon et al., 2017; Perera and Soares, 2017; Spentza et al., 2017; Nielsen and Jensen, 2011; Oikonomakis et al., 2019; Takami et al., 2021). In these kinds of studies, the main focus has traditionally been more on ship performances than on the topic of ship emissions, which have been treated less frequently and, in most cases, as an indirect consequence of fuel consumption. In recent years, the growing concern about atmospheric pollution brought the ship emissions topic under direct focus, with the consequence of a growing number of studies directly focused on it. A great concern is related to the effects of some of the pollutants on the climate system as Green House Gases (GHGs), and among these, the greatest focus is on CO_2. For a sound evaluation of such effects, the whole global shipping activities should be correctly evaluated and included in total CO_2 global budgets (Balsamo et al., 2021; Janssens-Maenhout et al., 2020; Bousserez, 2019; Crisp et al., 2015). Moreover, the direct effects of many pollutants on human health and on specific natural ecosystems are of great concern. For these topics, air quality modeling studies are needed, especially in correspondence with particularly sensitive land areas such as ports (with their surroundings) and coastal areas characterized by crowded coastal navigation.

1.4. Aim and contribution

In the present work, a detailed approach is adopted for assessing the ship performances, pollutant emissions, and the effects of the environmental conditions. On one side, a detailed treatment is adopted for modeling the evolution of ship performance and the consequent increment of emissions due to heavy weather, allowing a description of the intensity of pollution emissions sources, specifying "how much, where and when" these take place. On the other side, starting from such a quite precise specification of how much, where, and when, the atmospheric dispersion processes of the emitted pollutants are modeled, to estimate where (and when) they go. This modeling approach is too computationally intensive to be adopted in the construction of emissions inventories but could help to deepen the analysis of the involved dynamics, increase the awareness of the importance of several details, and allow the implementation of new and improved approaches for the simplified modeling to be adopted in this field.

In this framework, the authors have implemented and tested an integrated modeling system aimed at the realization of detailed along-route simulations of emission dynamics and the corresponding pollutant dispersion. The system can exploit the detailed meteo-marine data produced by mesoscale weather and wave forecasting models for simulating both ship performance and emissions and the latter's fate in the atmosphere.

The system is composed of the following modeling blocks:

- **Meteorological and wave forecast models**: to simulate the environmental metocean conditions in the area of interest, for a time interval covering the whole voyage duration.
- **Ship performance models**: to simulate the ship seakeeping responses and the corresponding powering performance and fuel consumption along the given route, by accounting for the main aero-hydrodynamic interactions with the environment, according to the metocean conditions from the first modeling block.
- **Propulsion Diesel engine and emissions models**: to obtain a detailed estimate of the main pollutants emission rates and whole route cumulates, based on the powering demand estimated by the second modeling block.
- **Pollutants dispersion model**: to simulate the fate in the atmosphere of the pollutants with local effects, by utilizing the emission rates, along route ship positions and timing, as estimated by the third module and in the same meteorological conditions from the first module.

After a description of the integrated modeling system, its functioning is analyzed by considering NOx, SO_2, PM10 and CO_2 emissions from a typical high-speed Ro-Ro ship with realistic meteo-marine conditions in two opposite case studies: one in nearly completely calm weather, and the other in heavy weather conditions.

This will demonstrate the various levels of analysis allowed by such a system regarding ship fuel consumption and the related main pollutants emissions. These range from the evaluation of emission rates along route profiles, with their linkage to the corresponding encountered metocean conditions, passing through the estimation of whole route emission cumulates, till to the generation of temporal sequences of density maps for the analysis of the space–time evolution of the atmospheric concentration values for all the studied pollutants, so as produced by the dynamical interplay between the ship specific technical details, and the realistic metocean conditions encountered along the route. The resulting picture is quite exhaustive and has a relevant potential for useful applications in diverse scientific studies, shipping management, and operational contexts, and we also foresee applications in the emission inventories field.

The rest of the paper is organized as follows. Section 2 gives a synthetic description of the state-of-the-art of the different modeling approaches adopted in our work. Section 3 gives a detailed description of the integrated emission modeling system developed in the present work. Section 4 gives an overview of the case study, describing the vessel, the propulsive system, and the commercial route under investigation. Section 5 discusses the results obtained, and finally, conclusions are drawn in Section 6.

2. Related works

In this section, a detailed state-of-the-art is reported for each one of the modeling blocks described in Section 1.

2.1. Meteorological and wave forecast models

In detailed Air-Quality studies over large areas, as in the cases implied by marine navigation, the more complete and convenient means to specify the environmental conditions is to use data from numerical meteo-marine hindcasting and forecasting models. Thanks to the use of sophisticated techniques (data assimilation techniques (Kalnay, 2003; Abarbanel, 2013)) to merge all the available observed data with the geophysical system physics implemented in the models, these data represent the optimal blending of observations and models, exploiting both the proximity to the real conditions from the former and the physical consistency and space–time uniformity from the latter. They are produced at forecasting centers by software chains composed of meteorological forecast models (Kalnay, 2003; Coiffier, 2011; Pielke, 1984), in which wind data are used to drive, in a one-way cascade mode, marine waves forecasting models (Komen et al., 1994; Cavaleri et al., 2007; Ardhuin, 2021). Moreover, forecast for wind and other atmospheric variables, characterizing atmosphere-sea fluxes through the air-sea interface, are used to force marine hydrodynamics models (Miller, 2007; Kämpf, 2010). As an improvement to these one-way cascade mode linked models' chains, two-way dynamically coupled atmosphere-waves-ocean modeling systems have been developed (Valcke et al., 2012; Ličer et al., 2016), and their application in operational forecasting contexts is promisingly growing. Modern meteo-marine hindcasting and forecasting models are full physics approaches, where most of the implied physical processes are explicitly modeled by the application of the Physics general principles for all the model-resolved dynamics. Only the finest unresolved scales are treated by semi-empirical approximations schemes or parameterizations. The global meteorological and oceanographic forecasting framework[1] is based on observing and modeling/forecasting components, all linked by highly efficient data transmission channels. The atmospheric modeling/forecasting component is composed of Global Models (GMs) and regional Limited Area Models (LAMs). On the one side, these latter, with their built-in detailed physics content (generally Mesoscale models (Pielke, 1984)), allow the simulation of atmospheric dynamics at quite a high resolution but at a relevant computational cost. Due to this, they are run on a "Limited" portion of the globe. Conversely, GMs are run at a coarser resolution with less explicit physics. Hence, they allow to cover the whole earth globe (Kalnay, 2003). GMs are operationally run by large international centers, and are initialized by a huge amount of quality checked observational data through sophisticated data assimilation techniques. This is only possible through large international collaborations, capable of timely collecting and processing a huge flux of global observed data (from ground stations and radars, vertical soundings, ships, buoys, aircrafts, and satellites)[2]. Each LAM model run mandatorily needs to be fed with boundary conditions from a GM run in order to guarantee the flux, through LAM boundaries, of information about the surrounding dynamics. Moreover, initialization data from GMs are a mandatory source of information from the observed conditions for defining the initial state of LAM model runs. In frontier research on LAMs, data assimilation techniques are also

[1] https://public.wmo.int/en/programmes/global-data-processing-and-forecasting-system

[2] https://public.wmo.int/en/programmes/global-observing-system

directly applied to them to improve the definition of their initial state, thanks to high resolution observational data, if and when available. On the other hand, the growth of computing power and the efficient blending of traditional modeling and data-driven machine learning techniques are progressively allowing global atmospheric simulations, with a seamless treatment of most of the dynamics from the large scale to very local ones, at quite high resolutions, before only reachable by LAMs (Buizza et al., 2022; Schneider et al., 2022; Bonavita et al., 2021). An analogous framework can also be described for oceanographic models (Pinardi et al., 2017; Moore et al., 2019). Wave forecasting models (Komen et al., 1994), if configured over enclosed marine basins, can be run without a strong need for boundary conditions for almost all the computational domains. In the case of wave forecasting over the Mediterranean Sea basin, the only boundary condition dependent areas are those around the two narrow inlets at Gibraltar and Dardanelles. For wave model run initialization, restart data generated by the antecedent run are generally used because wave motion is strongly wind driven and model non-linearity is not so effective in producing rapid forecast spreading. However, improvements in initial state definition can be attained by adding wave data assimilation stages (Lefèvre and Aouf, 2012; Houghton et al., 2022).

2.2. Ship performance models

A key algorithmic block for detailed and reliable estimation of emissions from a given ship at sea is the simulation of its performance. In particular, the task of such algorithms is to estimate the seakeeping and powering performance of the ship in relation to the meteo-marine conditions encountered along the route. Seakeeping performance is connected with the state of oscillatory motions of the ship in response to the encountered environmental conditions. Powering performance is connected to the functioning of the ship's main engine(s) and propeller(s), which ultimately determine the fuel consumption and the corresponding pollutant emissions. Seakeeping and powering performances are strongly related. The state of motion of the ship is caused by the interplay between the average ship speed and meteo-marine conditions, and it contributes to the total amount of resistance to be counterbalanced by the action of the engine-propeller system. In turn, at the same time, the feasibility of a given value of the average ship speed and the corresponding power requirement from the engine are determined by the capability and efficiency of the engine-propeller system to cope with the encountered meteo-marine conditions. Finally, the relevant outputs of powering performance computations, namely the required power and the corresponding engine(s) RPM rate(s), are the data required for a sound estimation of the pollutants emissions. This latter stage of the computation is done based on detailed engine models that are parameterized by the main engine type and corresponding constructor data sheets. The algorithms applicable in our approach to ship emissions computations are those originally developed for evaluating seakeeping and powering performance in ship design (Lewis, 1988) and that have also been adapted for weather routing applications. A hierarchy of different approaches has been developed for this, with different levels of accuracy and corresponding computational cost (Dern et al., 2016; el Moctar et al., 2021; Carlton, 2018). The techniques span from the complex and computationally heavy CFD (Computational Fluid Dynamics) and RANSE (Reynolds Averaged Navier–Stokes Equations) techniques (Kim, 2011; Tezdogan et al., 2015), able to simulate free surface and viscous phenomena (Kim et al., 2011) with high detail (but at a very relevant computational cost), passing through LES (Large Eddy Simulations) for propellers (Carlton, 2018), to arrive to time domain and frequency domain potential methods, that allow some savings in computational effort, due to opportune simplifying hypotheses on the characteristics of the involved fluids and their fluxes and interactions with ships structures at sea. For the goals of this study, the most complex algorithms cannot be applied due to their huge computational requirements. An acceptable compromise here is to work in a basically linear slender body approximation framework, adopting a strip theory. This is usually done in the preliminary phases of ship design and most of weather routing applications (Journée and Meijers, 1980; Grigoropoulos et al., 2003; Pacheco and Guedes Soares, 2007; Tsujimoto and Orihara, 2019; Zhang et al., 2020; Mittendorf et al., 2022; Orych et al., 2023). If necessary, the relevant non-linearities can be accounted for by ad-hoc addition of correction terms. A standard software suite for seakeeping is SMP (Conrad, 2005) and a benchmark study of several seakeeping software systems can be found in Gourlay et al. (2015), while interesting, more complex variants can be found in Parisella and Gourlay (2016), Veen and Gourlay (2012). Once computed the seakeeping state of a ship, in given environmental conditions, its powering state, i.e., the required power, engine RPM and ensuing fuel consumption rate, are estimated by accounting for the interplay between the hydrodynamic responses of the ship and the power available from the propulsion system, by applying standard powering computational algorithms (Carlton, 2018), i.e., as done in Yum et al. (2017). In recent years, the relevant pressure towards decarbonization in shipping brought a further push towards the development of innovative powering computational algorithms (ZeroNorth, 2022; Wartsila, 2022) by also exploiting Machine learning (ML) and Artificial Intelligence (AI) approaches, e.g. see Coraddu et al. (2017), Tay et al. (2021), Kim et al. (2020), Zhu et al. (2021), Lee et al. (2022). After the required power and corresponding engine RPM have been computed, accounting for the metocean conditions encountered in each way point of the analyzed route, an internal combustion engine simulation module can be run in order to perform detailed pollutants emission computations. In particular, in the following, we focus on Diesel engines (DEs).

2.3. Propulsion diesel engine and emissions models

For the majority of the vessels operating today, the main DEs, and to a lesser extent the auxiliary engines, are the main sources of emissions on-board (Baldi et al., 2014, 2015). Therefore, it is necessary to accurately estimate the main performance parameters and emissions from these energy sources. For this task, various computer modeling methodologies have been developed, able to represent the physical processes that occur in a DE under steady-state and transient conditions. Depending on the application requirements, mathematical representations of a varying range of accuracy and computational complexity are available in the literature, which are broadly classified into two categories (Grimmelius, 2003), including Physical Models (PMs) and Data-Driven Models (DDMs). PMs, rooted deeply in first principles, serve as the backbone for understanding complex systems by relying on foundational laws and core scientific principles. These principles could range from thermodynamics and fluid mechanics to combustion kinetics, ensuring that the models provide a comprehensive representation of the actual processes occurring within the engine. Due to their inherent accuracy and the depth of insight they offer, PMs have been the subject of extensive research over the years. Scholars and industry professionals alike have favored these models when it comes to engine performance investigations (Kalikatzarakis et al., 2021; Coraddu et al., 2021b; Tsitsilonis et al., 2023; Baldi et al., 2015). Their widespread acceptance is attributed to their ability to offer predictive insights, adaptability to different engine types, and the reliability of results, making them indispensable in both academic research and practical applications in the field of engine dynamics and performance optimization. Among those, the most widely employed are Mean Value Engine Models (MVEMs), which provide adequate accuracy in the prediction of most engine parameters while being computationally cheap (Malkhede et al., 2005; Guan et al., 2014; Theotokatos, 2010; Grimmelius et al., 2010; Theotokatos, 2008; Nikzadfar and Shamekhi, 2015; Geertsma et al., 2017; Theotokatos et al., 2018). More sophisticated approaches are zero-dimensional (0D) to three-dimensional (3D) models, which operate on per per-crank angle basis, allowing the calculation of time-varying parameters of the gas within the engine

cylinders during one crankshaft revolution (Wang et al., 2020; Xiang et al., 2019; Mohammadkhani et al., 2019; Sapra et al., 2020; Catania et al., 2011; Asad et al., 2014; Finesso and Spessa, 2014). Naturally, they are more computationally demanding than MVEMs, however, they can predict the detailed gas processes inside the cylinders with higher accuracy (Stoumpos et al., 2018, 2020). Several attempts to combine both approaches have also been proposed and utilized in a variety of applications, reportedly surpassing the predictive abilities of MVEMs with lower computational requirements than their 0D counterparts (Livanos et al., 2007; Ding et al., 2010; Baldi et al., 2015; Maroteaux and Saad, 2015; Tang et al., 2017). In general, state-of-the-art PMs achieve errors well within the tolerance margins provided by engine manufacturers in steady state conditions, whereas reported results during transient operations tend to be less accurate on average (Stoumpos et al., 2018). DDMs have been successfully applied in a variety of maritime applications, provided that the necessary quality and quantity of historical data is available. Most commonly employed for the prediction of emissions and performance of DEs are Artificial Neural Networks. There is universal agreement that DDMs can provide highly accurate results, at very low computational cost, w.r.t their PM counterparts. For instance (Nikzadfar and Shamekhi, 2014; Shin et al., 2020; Özener et al., 2013; Syed et al., 2017; Liu et al., 2018), all report errors lower than 3% in the prediction of most engine performance parameters and emission rates. In summary, PMs can adequately capture most process parameters of a DE under a broad range of operating conditions. However, there is a clear trade-off between accuracy and computational speed. The most accurate 3D models cannot run in real-time, whereas MVEMs lack accuracy, especially during transient operations. DDMs can provide highly accurate results with low computational cost, however, they can only be employed when the necessary amount of historical data is available.

2.4. Pollutant dispersion models

Numerical pollutant dispersion models can be split into the following categories: (i) Gaussian models, (ii) Eulerian models, and (iii) Lagrangian models.

(i) Gaussian models are based on a stationarity assumption for wind and turbulence and model pollutants emission in terms of point sources. Under these simplifying hypotheses, an analytical solution for the pollutants transport equation is available, in terms of Gaussian concentration plume (Stockie, 2011), that allows acceptable levels of approximation on the very local scale. Consequently, they are characterized by simplicity of application, do not require huge gridded input meteorological datasets, and can be run in very limited computational times also on portable devices. Due to these characteristics, Gaussian models are a standard for regulatory modeling in many environmental and industrial contexts and are also used both for on-site decision-making in emergencies and for estimating local scale effects due to long term continuous pollution emissions (Cimorelli et al., 2005; Holmes and Morawska, 2006; Leelőssy et al., 2018). On the other hand, it must be pointed out that their accuracy becomes scarce over spatial scales of a few tens of kilometers or in complex conditions (e.g., in complex orography or wind shear conditions).

(ii) Eulerian models allow the determination of the space–time fields of pollutants concentrations by solving the atmospheric transport equations, starting from the given initial conditions and imposing the appropriate boundary conditions. Moreover, they require a significant amount of data from Numerical Weather Prediction (NWP) models in order to define the atmospheric state and flux conditions during the whole simulation. The atmospheric transport equations are formulated using a set of space–time second-order Partial Differential Equations (PDEs) (Collett and Oduyemi, 1997). Due to the inherent complexity of such a system of equations, no general analytic solution is available, and numerical integration approaches are needed to solve these PDEs in the different application cases. Despite the availability of powerful numerical approaches, their solution is generally time consuming. Nevertheless, Eulerian models are used in decision support applications and environmental protection contexts. In order to optimize the computational times and accuracy requirements, such models are run in parallel computing architectures (Alexandrov et al., 2004; Dabdub and Seinfeld, 1996; Molnar Jr. et al., 2010), or adopting adaptive gridding (Garcia-Menendez and Odman, 2011).

(iii) Lagrangian particle dispersion models are based on a stochastic modeling approach, where the total released mass is subdivided into portions, generating a set of "Lagrangian parcels" whose positions must be determined to solve the pollutants transport problem. The evolution of each "Lagrangian parcel" is modeled as being composed of two contributions: the advection, implied by the local wind (whose field is obtained from an NWP model), and the turbulent random walk, corresponding to a Markow process described by the corresponding Langevin equation (Pozorski and Minier, 1998) as implied by the local turbulent state of the atmosphere. The solution of the resulting first-order stochastic Ordinary Differential Equations (ODEs), in terms of the time evolution of the positions of all the "Lagrangian parcels", determines the time evolution of the pollution spatial pattern. The computational cost of a Lagrangian model implementation depends on the number of parcels whose stochastic motion has to be computed. In many cases, a sufficiently good first guess approximation of the main direction of pollution dispersion can also be obtained with a small number of parcels. A further common approximation is obtained by neglecting the turbulent diffusion term and computing the deterministic trajectories as implied by the large-scale wind (Neroda et al., 2014). This provides a quick outlook on the main pathway of pollution dispersion, allowing a first quick estimate of the more likely affected areas, without using a computationally heavy large domain Eulerian model or a time consuming solution, a fully stochastic Lagrangian model with many particles.

Mixed approaches have also been developed, such as Lagrangian–Eulerian or Lagrangian–Gaussian hybrids. An example of such hybrids is offered by the puff models (Draxler and Hess, 1998; Thykier-Nielsen et al., 1999), i.e., Gaussian–Lagrangian models where spatially extended Gaussian puffs substitute the "Lagrangian parcels". In such hybrid models, the motion of the puff is simulated with Lagrangian algorithms, and the turbulent spread of the distribution, internal to each puff, is modeled in terms of a Gaussian-like parameterization. The final superposition of all the modeled puffs, each with its Gaussian spreading, determines the pollution concentration results. Within a puff, the assumptions of the Gaussian model must hold. Therefore, a puff splitting algorithm is applied within each puff to limit errors caused by the increasing puff size, thus guaranteeing the conditions of applicability of the Gaussian approximation (Draxler and Hess, 1998).

3. The integrated modeling system

The integrated simulation modeling system developed in this work is composed of four stages and is reported in Fig. 1

- **First stage** - Environmental metocean conditions: consists of generating detailed data using state-of-the-art meteorological and wave forecast models.
- **Second stage** - Ship performance along the route: data from metocean models (in particular wind and seaway conditions) are used to compute the ship performance in correspondence with each way point of the considered route.
- **Third stage** - Ship emissions: powering performance data are used to compute the ship emission rates of the relevant pollutants, in correspondence with each way point of the route.
- **Fourth stage** - Pollutant dispersion: emission rates together with the same atmospheric forecast data, are used to feed state-of-the-art pollutant dispersion models to evaluate the corresponding evolution in the atmosphere of each modeled pollutant.

A detailed description of each modeling stage is given below.

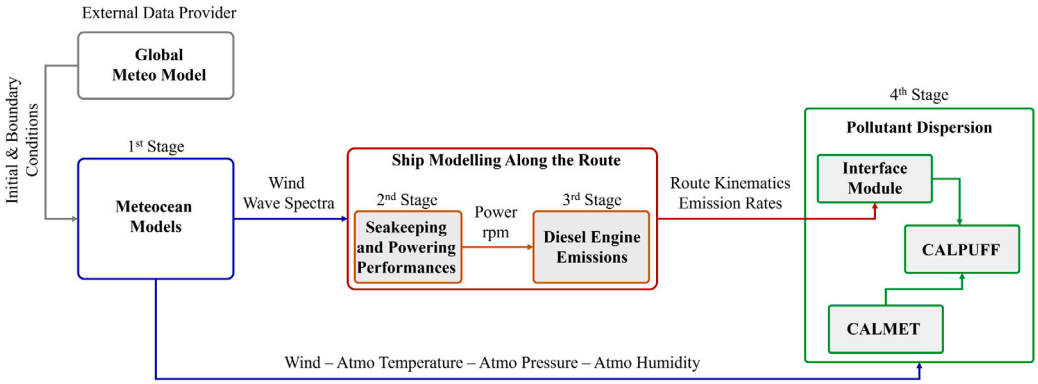

Fig. 1. Scheme of the four stages of the integrated modeling system. Left (blue): 1st stage, metocean models. Center (red): 2nd and 3rd stages, ship performance and emission models. Right: 4th stage, pollutant dispersion models. Data flux is schematically indicated along connecting arrows.

3.1. First stage: metocean conditions

In this work, the authors used meteo-marine data from the Consorzio LaMMA operational forecasting system.[3] The meteorological component is based on the mesoscale meteorological Weather Research and Forecasting (WRF) model,[4] with initialization and boundary conditions from the American global model (National Oceanic and Atmospheric Administration, National Centers for Environmental Prediction (NCEP), Global Forecast System (GFS)). The post processing stages of the WRF model allow the output of a wide range of meteorological variables, starting from the standard prognostic ones wind, pressure, temperature, and humidity (defined over the whole computational area and on all the model height levels) till to several derived quantities, typically utilized in the operational weather forecasting practice. The standard prognostic variables at the lowest model output levels are those needed for driving the other models in the integrated chain described in this work. In particular the wind, at the standard height of 10 m, is used as the main forcing for the wave forecasting model, while for the air quality modeling stages atmospheric vertical profiles of wind, temperature, pressure and humidity are needed. Consorzio LaMMA wave forecasts used in this system are generated by running, in cascade with respect to WRF model runs (i.e., by using 10 m wind data from it), the third-generation spectral wave model Wavewatch III[5] (WW3) (Tolman et al., 2009). The resulting wind-wave forecasting operational chain is run two times a day (initialization at 00: 00 and at 12: 00 UTC) over the whole Mediterranean Sea (WW3) (Tolman et al., 2009) for the next five days at a resolution of about 12 Km. The post processing stages of WW3 model allow the output of many wave forecast parameters over the whole computational domain. These comprise the wind from WRF model, the standard (spectrum averages) quantities such as significant wave height, mean wave period and direction. Moreover, it is also possible to have the output of the complete wave spectrum (discretized over the model frequency-direction computational grid) in correspondence with user-required points. Of all these data, the integrated system utilizes wind and whole spectral data over all the route's way-points to drive the computation of ship seakeeping and powering performance along each route. The flux of the main data streams in the integrated system, schematically illustrated in Fig. 1, will be further described in the next sections devoted to the other stages.

[3] http://www.lamma.rete.toscana.it/mare/modelli/vento-e-mare
[4] https://www.mmm.ucar.edu/weather-research-and-forecasting-model
[5] https://polar.ncep.noaa.gov/waves/wavewatch/

3.2. Second stage: ship performance along the route

The ship performance along a given route is computed through the SPAR (Seakeeping and Powering Along a Route) computational suite. It has been developed in Orlandi and Bruzzone (2012), Orlandi (2012) and subsequently applied in weather routing related studies (Orlandi et al., 2015). It is composed of a main procedure that drives the whole computation process along with the WayPoints (WP) of a given route by extracting wind and wave data at the correct space–time positions. These are used to perform seakeeping and powering computations. The main idea implemented in SPAR is that the propulsive engine load and the consequent propulsive requirements are evaluated through the dynamic balance between propeller(s) thrust and ship's total resistance by powering computations, implemented by applying standard algorithms (Carlton, 2018; Coraddu et al., 2014). In this process, the total resistance of the ship is evaluated by considering the effects of the environmental conditions through seakeeping computations. The SPAR algorithm outputs a set of data for each WP of the route. Many of them are useful for weather routing applications, e.g., significant amplitudes of seakeeping motions, main components of ship resistance, and corresponding fuel consumption rate. The SPAR output variables most relevant for the computation of ship emissions are the required power and propeller RPM rotational speed, characterizing the equilibrium working point of the engine and propeller (Orlandi, 2012) in correspondence of the powering load due to the total resistance, computed for each WP. SPAR allows the simulation of different powering configurations, like different numbers of active engines and different propeller pitch values. This latter possibility has been exploited to investigate the feasibility of metocean dependent combinator settings in Coraddu et al. (2012). It was a preliminary study whose implementation had the potential of adding a further level of optimization for the powering conditions of ships equipped with CPP. Seakeeping computations in SPAR are based on the strip theory (Ogilvie and Tuck, 1969), in particular, a modified version of the Public-Domain Strip (PDSTRIP)[6] program (Bertram et al., 2021) is used (PDSTRIP-SPC) (Orlandi, 2012) that allows the computation of significant responses by using numerical directional wave spectra from WW3 model, thanks to the fact that the general framework of strip theory (Bertram, 2011) is compliant with the linear wave superposition approximation implied by the adoption of a spectral approach (Price, 1974). In SPAR, the total ship resistance is evaluated in terms of the standard decomposition with three main components as reported in Lewis (1988), according to Eq. (1):

$$R_T = R_{hull} + R_{aw} + R_{wind} \tag{1}$$

[6] https://sourceforge.net/projects/pdstrip/

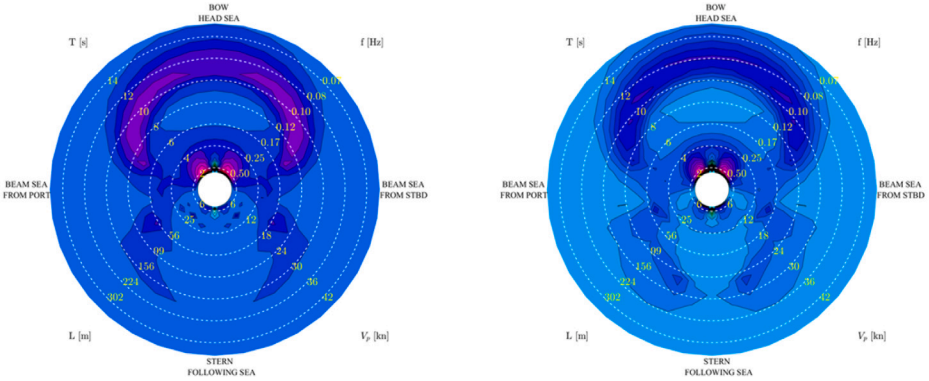

(a) ARO function - Speed of 18 kn. (b) ARO function - Speed of 24 kn.

Fig. 2. Added Resistance in waves Operator *ARO* computed by PDSTRIP-SPC (Orlandi, 2012).

where R_{hull} is the calm-water resistance (Birk, 2019) that depends on ship hull form, hull appendages, loading and trim conditions (Reichel et al., 2014), and speed through water, R_{aw} is the added resistance in waves (Blendermann, 2013), due to the hydrodynamic interaction of the ship with the field of the encountered marine surface waves, and where R_{wind} is the wind added resistance (Lewis, 1988), due to the interaction of ship superstructures with the surrounding air. In PDSTRIP-SPC, the value of R_{aw} for generally confused seaways is numerically computed in terms of the frequency-directional integral of the product of the Added Resistance Operator (ARO) and the directional wave spectrum from the WW3 model, according to Eq. (2):

$$R_{aw} = 2\int_0^{\infty}\int_0^{2\pi} ARO\left(\omega,\theta_{raw}\right) S_{\zeta}\left(\omega,\theta_{raw}\right) d\theta_{raw} d\omega \tag{2}$$

where $ARO(\omega,\theta_{raw})$ is the longitudinal component of the drift force in regular waves per (regular) wave amplitude squared (Faltinsen, 1993), $S_{\zeta}(\omega,\theta_{raw})$ is the directional wave spectrum, and the integration variables (ω, θ_{raw}) are the wave angular frequency and the ship-relative wave direction. The ARO functions are strongly vessel dependent and must be evaluated for the specific vessel loading conditions and each value of the speed through the water in the speed range of interest. In Fig. 2, examples of the ARO function computed by PDSTRIP-SPC for the vessel described in Section 4 are reported. In particular, the ARO polar diagrams computed for a speed through the water of 18 and 24 knots are shown in Fig. 2(a) and (b), respectively. These have been computed on a grid of wave directions in the 0–360° interval, with steps of 10°, in the azimuthal direction and wave period values in the radial direction, covering the interval from 3 to 18 s (radial coordinates, green circles every 2 s). The obtained results are in good accordance with other literature results (Matulja et al., 2010).

The wind added resistance term depends on the total ship-relative wind $\mathbf{U}_r$, resulting from the vector composition of the ship speed over the ground with the wind due to meteorological conditions, and can be evaluated according to Blendermann (2013) in terms of:

$$R_{wind} = \frac{1}{2}\rho_{\text{air}} A_T U_r^2 C_x\left(\theta_{\text{wind}}\right) \tag{3}$$

where ρ_{air} is the air density, A_T is the ship frontal area, and U_r is the modulus of the ship-relative total wind vector. The longitudinal wind resistance coefficient $C_x\left(\theta_{\text{wind}}\right)$ depends on the ship above waterline structures and is a function of the ship-relative wind angle θ_{wind}. The vessel-specific C_x coefficients can be experimentally estimated from wind tunnel (Wang et al., 2019) or numerical simulations by means of Computational Fluid Dynamic analyses (Saydam and Taylan, 2018). In recent research activities, a different approach to ship performance estimation has been developed based on the decoupling of the heaviest computational tasks, both for seakeeping and powering properties of the ship, from the computationally lighter evaluation of ship performance in correspondence with each particular metocean condition. This decoupling is based on the pre-calculation of Look-Up Tables (LUTs) where ship-specific aero-hydrodynamic and powering coefficients are computed and stored once and for all and whose utilization for ship performance evaluation in realistic metocean require only light computational tasks. This LUTs-based computational approach, as described in Orlandi et al. (2021, 2022), has already been implemented in a prototype ECDIS interface in the general framework of e-navigation and also performing rough numerical tests for sail-assisted ships (Orlandi et al., 2022). It could be further extended to estimate ship emissions, trying to exploit its potentialities in combining a good level of modeling details with a quite low computational cost to allow a quite detailed accounting of meteocean contributions to pollution emission dynamics also in the context of computationally intensive practices as for the construction of emission inventories. Furthermore, utilizing a modular approach, especially one grounded in LUTs, aligns seamlessly with the burgeoning integration of machine learning and big data techniques in ship modeling. This synergy allows for a more dynamic and adaptive framework, catering to maritime simulations' evolving complexities and demands. For more insights and applications in this realm, refer to Guachamin-Acero and Portilla (2022), Taskar and Andersen (2021). Moreover, a modular approach, as this is based on LUTs, could be fit to be integrated with the growing application of machine learning and big techniques in ship modeling.

3.3. Third stage: ship emissions

Accurate evaluation of the emissions, particularly in NO_x formation, requires detailed modeling of the physical processes occurring in the vessel's Diesel engines. In the subsequent sections, we provide a comprehensive overview of the Diesel engine modeling approach for thoroughness. A more detailed explanation and validation results can be found in Kalikatzarakis et al. (2021).

The Diesel engine model for the vessel has been designed using a modular approach, as displayed in Fig. 3. This model is not simplistic; it encompasses a multitude of key variables that are integral to accurately representing an engine's operation. Among the inputs, geometric engine data accounts for physical attributes like the size of the cylinder, piston stroke length, and other key measurements that affect engine operation. Intake and exhaust valve profiles are also crucial, as they dictate the timing and degree of air and exhaust gas flow, impacting engine performance. The performance maps for the compressor and turbine contribute to the model by demonstrating the relationship between the input variables (like pressure, temperature, and speed) and output performance. Additionally, the waste gate's geometric details and control information are vital in modulating the engine's boost pressure and ensuring optimal performance. The engine sub-model constants play a significant role in predicting the engine's

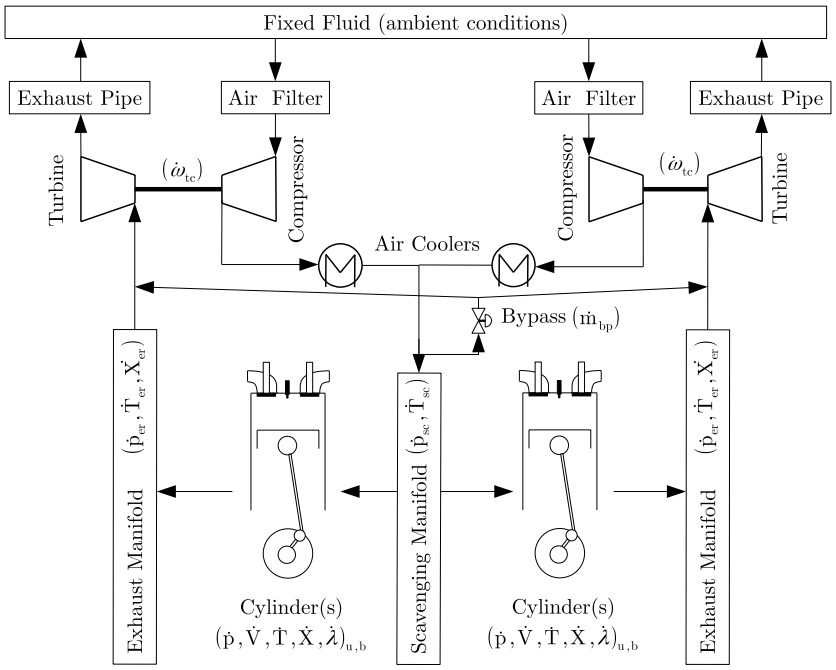

Fig. 3. Modeling approach of the Diesel engines.

operational efficiency. These include combustion constants that predict fuel consumption and emission rates, heat transfer constants that evaluate the engine's thermal management, and friction constants that quantify the engine's mechanical losses. To simulate the engine's real-world operating environment, the model takes into account the engine's operating condition (load/speed), which is critical for defining the engine's output power, and the surrounding environmental conditions, such as ambient temperature and pressure, which can significantly impact the engine's performance. Lastly, the model also necessitates initial conditions for the working medium. These conditions relate to the temperature, pressure, and composition of the gases (like air and exhaust gases) in the engine's cylinders, pipes, and receivers at the start of the simulation. These parameters are pivotal in initializing the engine simulation and ensuring its accuracy. The elements within the engine, such as the scavenging air (sc) and exhaust gas receivers (er) are simulated as flow receiver components, functioning as control volumes. Components, including the compressor, air cooler, cylinders, and turbine are represented as flow elements in the model. The peripheries of the engine are modeled using fixed fluid elements, maintaining consistent pressure and temperature. In order to compute the rotational speed of the turbocharger and crankshaft, shaft elements are employed in the model. The engine governor plays a crucial role in modulating the fuel rack position and integrating the necessary fuel rack limiters, thus controlling the engine's fuel injection and speed. The properties of the air and exhaust gas have been considered functions of various factors, namely temperature (T), fuel-air equivalence ratio (λ), and their composition (X). Essential constituents such as oxygen, nitrogen, carbon dioxide, and steam are considered for determining the exhaust gas composition.

Every flow element in the model utilizes the open thermodynamic system concept (Watson and Janota, 1982; Heywood, 1988), taking pressure (p), temperature, and the properties of the working medium from adjacent elements as inputs. This concept aligns with established studies on turbocharging and internal combustion engines (Casey and Robinson, 2013). Subsequently, mass ($\dot{m}$) and energy flow rates entering and exiting each element are calculated based on mass and energy conservation principles. These flow rates then serve as inputs for adjacent flow receiver elements. Torque outputs, on the other hand, function as inputs for shaft elements. These shaft elements compute the rotational speeds of the turbocharger (ω_{tc}) and propulsion plant shafts, employing angular momentum conservation.

The compressor model leverages its steady-state performance map, estimated through the methodology outlined by Casey (Casey and Robinson, 2013), while the turbine model incorporates its swallowing capacity and efficiency map. Pressure losses within the air cooler and air filter are related to the air mass flow rate, which also affects the effectiveness of the air cooler. In the scavenging air receiver model, heat transfer is not considered, contrasting with the exhaust gas receiver, where heat transfer to the ambient environment is computed. This computation is based on the overall heat transfer coefficient, employing a Nusselt–Reynolds number correlation for gas flowing within the pipes, as referenced in Rohsenow's 1985 handbook (Rohsenow and Hartnett, 1988). Additionally, pressure losses within the exhaust gas receiver are contingent on the exhaust gas mass flow rate.

The in-cylinder process utilizes a two-zone, zero-dimensional model as articulated by Merker et al. Merker et al. (2005).

This model operates on a crank-angle basis, facilitating a detailed per-cycle analysis of the engine's crank rotation. This analysis employs the mass and energy conservation equations, alongside the gas state equation, solved in their differential form. This methodology allows the computation of various parameters within the engine cylinders and manifolds, including pressure, volume, temperature, and gas composition. Combustion is represented via a two-zone model, delineating a zone containing combustion products and an unburned mixture zone, again as proposed by Merker et al. Merker et al. (2005). The Woschni heat transfer model, originating from Woschni (Woschni, 1967), and extensively applied in a wide array of studies, is utilized to determine the in-cylinder gas-to-wall heat transfer coefficient. Finally, the heat release rate simulation adheres to the Vibe model, as outlined in Merker et al. (2005).

The evaluation of combustion products utilizes the method delineated by Rakopoulos et al. Rakopoulos et al. (1994). It is based on a chemical equilibrium scheme that considers 11 species, obtained from 7 equilibrium equations and 4 linear atom balance equations. This method is chosen due to its reported accuracy, small computational cost, and validity against any fuel, expressed by the general chemical form $C_xH_yO_zN_w$ (Rakopoulos et al., 1994; Kalikatzarakis et al., 2021; Coraddu et al., 2021b,a, 2018; Hanson and Salimian, 1984). It is worth

noting that our study, which forms the foundation for broader research, centers on key pollutants identified by current regulatory standards, namely: NOx, SO_2, PM10, and CO_2 as reported in Tables 4 and 5 and their evaluation have been carried out in accordance with the work of Diesch et al. (2013), Winnes and Fridell (2009), Di Natale and Carotenuto (2015).

3.4. Fourth stage: pollutant dispersion

The adopted pollutant dispersion modeling approach is based on the CALMET (Scire et al., 2000a) and CALPUFF (Scire et al., 2000b) model system. CALMET is a diagnostic meteorological model that provides hourly three-dimensional input fields to the Lagrangian dispersion model CALPUFF. It plays the role of the numerical interface needed to process the data from a generic meteorological forecasting model to allow them to be properly utilized by CALPUFF. In the present implementation, such data are generated by the WRF meteorological model as described in Section 3.1, and consist of wind and air temperature, pressure, and humidity as shown schematically in Fig. 1 (blue arrow entering the fourth stage block). The tasks performed by CALMET consist not only of mere interpolations but also require modeling to guarantee dynamical consistency. CALPUFF simulates the non-steady-state transport, dispersion, removal, and chemical transformation of air pollutants and calculates hourly concentrations at specified receptor grids. This approach has already been proposed for the study of ships emissions, as reported in Toscano et al. (2021), He et al. (2021), Murena et al. (2018), Poplawski et al. (2011).

CALMET and CALPUFF are configured on a common computational domain with the same resolution, and they operate with a terrain-following vertical coordinate system. In the proposed configuration, the horizontal spatial resolution is 9 Km, and in the vertical dimension, there are 14 levels from 10 to 4,500 m, more densely spaced at the lower surface.

The input for CALPUFF is completed by pollutants sources data, which are characterized in terms of ship kinematics and the respective emission rates, as schematically indicated in Fig. 1 (red arrow entering the fourth module block). In the present modeling approach, the ship emission process is schematized by sequentially activating a point source for each route Way-Point (WP), namely Emission Way-Point (EWP). Each EWP is activated when the ship passes it, in accordance with route kinematics (i.e., ship speed of advance and along-route distances). To fit with the time resolution needed by CALPUFF, emission rate data on EWP are obtained by linear interpolation of ship performance data from SPAR on the route's WPs. The pollutants modeled in the fourth stage are those that can have a relevant local impact, i.e., NOx, SO_2 and PM10, whose Emission Rates (ERs) have been estimated, for each EWP, as described above. For such pollutants, the output stage of the fourth module allows the production of spatialized maps of concentration, that convey a relevant piece of information for evaluating their impact at the local level.

3.5. Overall system implementation

The whole integrated system, as described above, is characterized by the extensive use of various models, both covering a wide range of dynamical scales and touching several different scientific and engineering disciplines. The main goal of the work reported here was to demonstrate the feasibility of such a system and the richness of the data that can be obtained through it. The analysis of the case studies reported in the following paragraphs will illustrate such features.

It must be added that the whole system has been implemented by adopting state-of-the-art models and widely used computational approaches (albeit with some original developments) in order to allow a high level of applicability. The geophysical model components (i.e., meteorological, waves, and pollution dispersion models) have been implemented by utilizing well documented open source suites, that are the result of decades of sound international scientific investigation in universities and research institutions, with countless validated operational implementations around the world (as can be seen from the references cited in Sections 3.1 and 3.4). The ship specific modeling components are based on well documented common approaches in naval architecture and marine engineering, with some relevant novelty features, that are well documented in the author's publications referred to in Sections 3.2 and 3.3. The integrated implementation of the whole system is, however, replicable, albeit the work of a multidisciplinary team with working experience in the specific fields is required, and enough computational power is needed for useful applications. Once implemented, such a comprehensive system brings detailed ship performance computing approaches used in ship design to be available for pollutant emission and dispersion studies. This allows us to analyze the roles of the different environmental and technological components with a level of detail not available in the commonly used methods in the fields of emissions and inventories. A further very relevant distinctive feature of the system is that it gives full control of all the components, allowing the analysis and fine tuning of all the modeling blocks to obtain the best results by reducing the main errors and their combined effects. It must be pointed out that every study or investigation devoted to environmental dynamics and the effects of "technological assets" on the environment have, as an unavoidable and inherent feature, the need to cope with a wide range of potential uncertainties interacting between them and affecting the final results. The main features of this are schematically summarized below.

- Environmental data: they are needed, but cannot be taken solely from observations, due to the lack of uniform space–time coverage of these latter. Data from metocean numerical models are best suited under this respect but such models are strongly non-linear, with sensitive dependence on initial conditions. Taking them from "external" providers potentially opens a gap of uncontrolled source of errors. Some consequences of this have been investigated in a recent work, in collaboration with one of the authors (Bulian and Orlandi, 2022), in a slightly different field, but with strong analogies with the present study. Hence, the complete control over the whole chain of models allows to reduce many of the uncontrolled sources of data spreading, with the exception of the unavoidable boundary and initial conditions from Global Models. These latter are from very reliable international meteorological centers.
- Technological assets: in some cases, their models exhibit less complex behavior, but a quite high level of detail is needed to treat them in realistic conditions. However, the behavior of marine systems, like ships, is strongly affected by the nonlinearities brought in by their hydrodynamic components (Guedes Soares, 1991; Parunov et al., 2022; Mittendorf et al., 2022; Abdelwahab et al., 2023), and by the thermo-fluid dynamics of the engines. Hence, the capability to model many details and to tune the detail level will be a strength point in further developments of the system.
- The predictability limits of complex non-linear systems, as for metocean environmental conditions, change with the system state, so as it is itself considered as a prognostic variable. Due to this, one of the main trends of metocean prediction is towards probabilistic approaches, where the predictability of complex non-linear systems is tackled by "ensemble techniques" (Council, 2012; Kalnay, 2003). A first investigation with such an approach has been performed by the authors (Orlandi et al., 2015), and it will be exploited in future developments.

The reliability and the limitations of the single model components of the system have already been tested in the context of research studies and of the operational activity of Consorzio LaMMA.[7,8] The further step,

[7] https://www.lamma.toscana.it/modelli/modelli-atmosferici
[8] https://www.lamma.toscana.it/mare/modelli/ww3-info-sul-modello

Table 1
Main vessel characteristics.

Main particulars	Unit	Value
Full load displacement (Δ)	[t]	15,470
Length between the perpendiculars (L_{pp})	[m]	160
Beam (B)	[m]	25
Propeller diameter (D_p)	[m]	5
Max pitch (P_p)	[m]	7.134
Number of blades (Z)	–	4

Table 2
Main engine characteristics.

Engine characteristics	Unit	Value
Model	–	Wärtsilä 12V46C
Power output at MCR[a]	[kW]	11,700
Cylinder number	–	12
Engine speed	[rpm]	500
Bore	[mm]	460
Stroke	[mm]	580

[a] Maximum Continuous Rating.

after the presently described feasibility investigation, will be a thorough test and tuning phase, where the error characteristics of the whole integrated system will be investigated, and its performance will be optimized. In this phase, the systematic comparison with high quality observed data will be of the greatest preminence, regarding both environmental data[9] and in-service measurements of ship performances. Comparisons with detailed studies of the impact of specific ship emissions on coastal areas and islands, such as those in Becagli et al. (2012, 2017), will also be performed and will help to test and tune the system. In this phase of the study, the complex interrelations between the metocean background states, the local atmospheric boundary layer conditions, and the different contributions of ship traffic emissions will be accounted for.

4. Case study description

In this section, the authors describe the case study vessel and three different routes for which the powering performance and the corresponding pollutant emissions will be forecasted. For these forecasts, realistic meteo-marine conditions have been utilized through metocean data from Consorzio LaMMA operational forecasting models, as described in Section 3.1. Two scenarios have been studied characterized by differing metocean conditions: a calm weather case and a heavy weather case.

In this work, the availability of a quite complete dataset regarding a real RoPax ship has been exploited consisting of ship plans and sections, hydrostatics, and loading, propellers, and engines. Such data enabled, in the context of precedent studies (Orlandi et al., 2015), the generation of most of the input needed to build the models and feed the SPAR Algo, as described in Section 3.2. In particular, the vessel under investigation is equipped with four Wärtsilä 12V46-C engines and two controllable pitch propellers. With the installed propulsive power, at 100% load (i.e., 11,700 kW for each of the 4 engines, at 514 rpm), the vessel is capable of reaching 28 knots of maximal speed. The main particulars of the vessel are reported in Table 1, while the characteristics of the engines are presented in Table 2.

The diesel engine power and fuel consumption rate are evaluated according to standard algorithms as described in Section 3.2. The case study vessel is simulated as performing the voyage from Genoa (Italy) to La Valletta (Malta), taking into account two different speeds (i.e., 18 and 24 knots), along three different routes, Route 00, Route O1, and

[9] In-situ and satellite data from: https://data.marine.copernicus.eu/products

(a) Route 00.

(b) Route 01.

(c) Route E1.

Fig. 4. Case Study routes.

Route E1, as reported in Fig. 4. Route 00 (Fig. 4(a)) is the central and shortest one, Routes O1 (Fig. 4(b)) and E1 (Fig. 4(c)) are Western and Eastern variants of it, respectively. In Table 3 the voyage data is summarized.

4.1. Calm weather scenario

In this scenario, the weather conditions correspond to the departure time on 27th August 2015 at 12:00 UTC. In Fig. 5 the significant wave height (H_s) maps together with the corresponding wind fields are

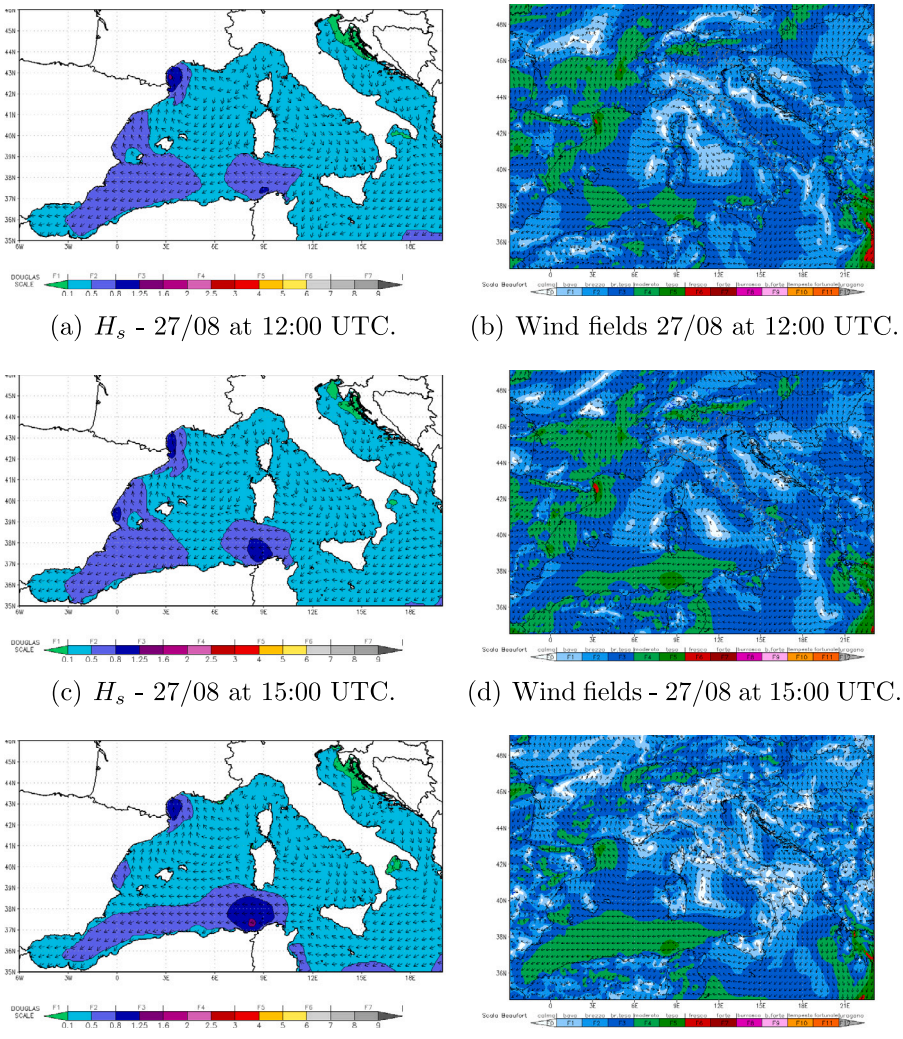

(a) H_s - 27/08 at 12:00 UTC. (b) Wind fields 27/08 at 12:00 UTC.

(c) H_s - 27/08 at 15:00 UTC. (d) Wind fields - 27/08 at 15:00 UTC.

(e) H_s - 27/08 at 21:00 UTC. (f) Wind fields 27/08 at 21:00 UTC.

Fig. 5. Calm Water Scenario.

Table 3
Voyages data.

Ship Speed [kn]	Route Length [NM]	Voyage Duration [h]
Route 00		
18	585.2	32.5
24		24.4
Route O1		
18	610.6	33.9
24		25.4
Route E1		
18	641.1	35.6
24		26.7

reported for 27th August at 12:00 UTC (Figs. 5(a) and 5(b)), 15:00 UTC (Figs. 5(c) and 5(d)), and 21:00 UTC (Figs. 5(e) and 5(f)).

From the figures, it is possible to observe the consequences of the presence of a high pressure configuration over the Mediterranean area, with the main maximum pressure located at the center of the Tyrrhenian Sea. The resulting circulation was anti-cyclonic (clockwise) with a very weak wind pattern and calm conditions, except for the area of Sardinia Channel and surroundings, where relatively stronger winds are present due to dynamic intensification.

4.2. Heavy weather scenario

In this scenario, the weather conditions correspond to the departure time on 1st October 2015 at 16: 00 UTC. In Fig. 6 the significant wave height maps together with the corresponding wind fields are reported for three different times on 2nd October, 09:00 UTC (Figs. 6(a) and 6(b)), 12:00 UTC (Figs. 6(c) and 6(d)), and 15:00 UTC (Figs. 6(e) and 6(f)).

In this case, the scenario is characterized by a very deep and concentrated low pressure system over the Central Mediterranean Sea. Its center spanned both Sardinia and Corse Islands, generating strong winds and rough sea conditions. At the time of Fig. 6, the low pressure center was over Corse Island. Due to the cyclonic circulation, wind and waves direction was from Southern quadrants over the Tyrrhenian Sea, and from Northern quadrants over the Ligurian and Corse Sea. These metocean conditions generate significant head wind and head waves along each one of the three studied routes. Differences between the voyages are introduced by the different voyage timing and traversed sea areas corresponding to each route and each selected ship speed value.

5. Results analysis and discussion

In this Section, the results obtained with the integrated modeling system described in Section 3, applied to the two scenarios of the case

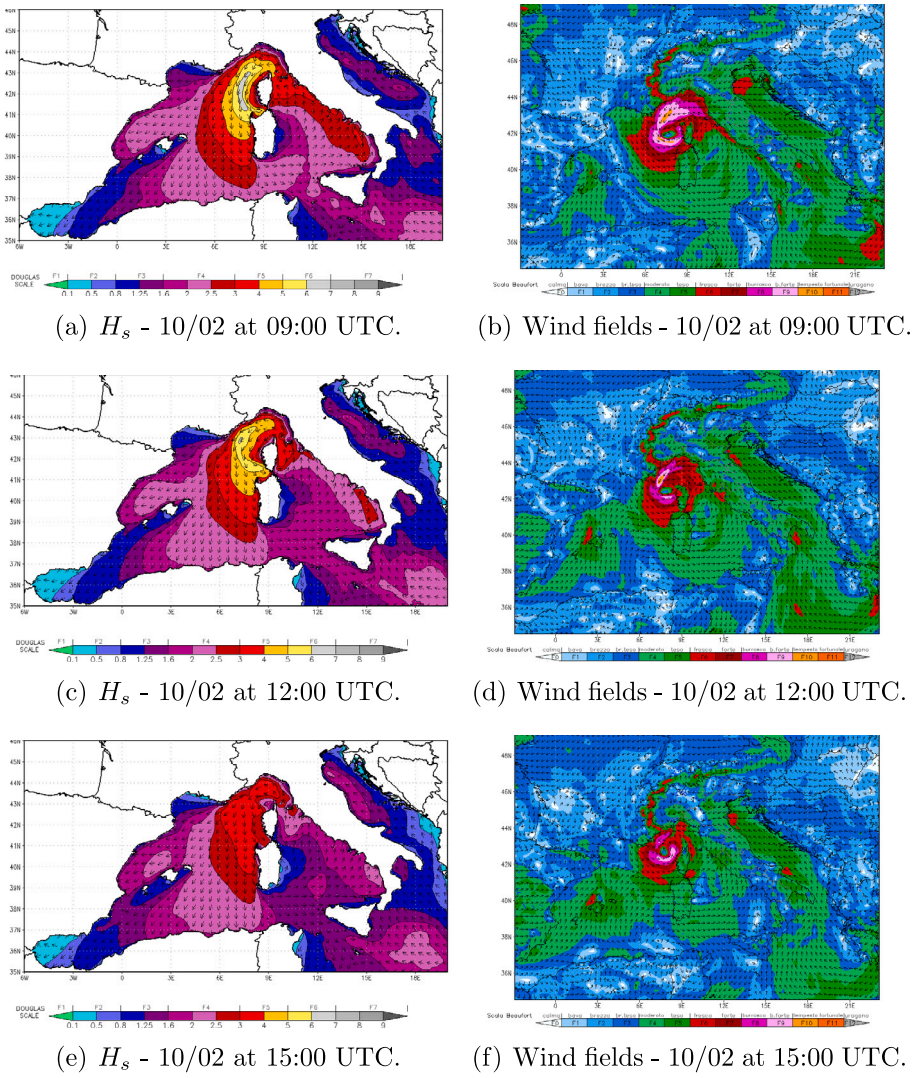

(a) H_s - 10/02 at 09:00 UTC. (b) Wind fields - 10/02 at 09:00 UTC.

(c) H_s - 10/02 at 12:00 UTC. (d) Wind fields - 10/02 at 12:00 UTC.

(e) H_s - 10/02 at 15:00 UTC. (f) Wind fields - 10/02 at 15:00 UTC.

Fig. 6. Heavy Weather Scenario.

study proposed in Section 4 are reported and discussed. In Tables 4 and 5 the main results of emissions simulation for the Calm Water and Heavy Whether scenarios are presented. More specifically, the total fuel consumption, total emitted NO_x, SO_2, PM_{10} and CO_2 are reported for ship speed values of 18 and 24 knots and for all voyages of the vessel under examination.

In particular, in the Calm weather scenario, the total ship resistance R_T is essentially given by the calm water term R_{hull} plus a wind added resistance term R_{wind} solely due to the ship speed. In the Heavy Weather Scenario, for the most part of each voyage on all the routes, heavy head wind and sea conditions are present, with a relevant increase of R_T, due to a greater R_{wind} and a due to very relevant values of the added resistance in waves R_{aw}. As a consequence, the heavy weather causes a significant increase (w.r.t. the calm weather scenario) in fuel consumption. In particular, it amounts to about 17% and 18% along Routes 00 and E1, respectively, while along route O1, we have a lower 11% value, thanks to the partial sheltering effect of Course and Sardinia Islands. The computed pollutant emissions also show a corresponding relevant increase due to heavy weather.

It is worth noting that the figures presented in Tables 4 and 5 are vessel-specific, shedding light on the actual emissions under certain operational conditions of the particular ship under investigation. This level of specificity contrasts with the broader, averaged character of data in reports such as e.g. Cooper and Gustafsson (2004), Smith et al. (2014). The averaging process adopted in such studies offers a general guideline on typical emission data values but does not account for the nuanced variations from vessel to vessel or from machinery type to machinery type and might not accurately represent specific meteo-marine scenarios, such as those our vessel operates under. Focusing on specific vessel data makes it possible to obtain a clearer and more precise understanding of emissions in particular contexts. The results of the pollutant dispersion model for the Calm Water and Heavy Weather

Table 4
Calm Weather Scenario results, computed total values of: fuel consumption, and emitted NO_x, SO_2, PM_{10} and emitted CO_2, for each route and at each ship speed.

Ship Speed [kn]	Total Fuel [t]	Total NO_x [kg]	Total SO_2 [kg]	Total PM_{10} [kg]	Total CO_2 [t]
Route 00					
18	81.78	5636.2	3430.7	489.2	251.6
24	108.96	7767.8	4728.2	674.3	338.1
Route O1					
18	86.04	5945.4	3619.0	516.1	264.6
24	114.38	8139.8	4954.7	706.6	354.9
Route E1					
18	88.32	6100.8	3713.5	529.6	271.6
24	117.96	8363.8	5091.0	726.0	365.9

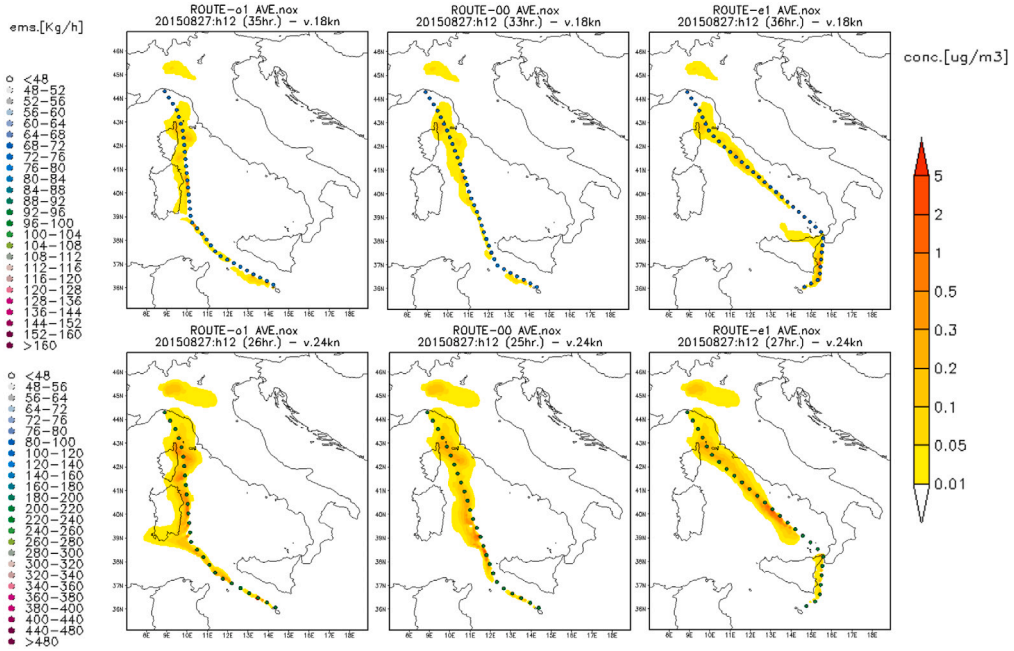

Fig. 7. Calm Weather: average values of computed of NO_x concentration.

Table 5
Heavy weather scenario results, computed total values of: fuel consumption, and emitted NO_X, SO_2, PM_{10} and emitted CO_2, for each route and at each ship speed.

Ship Speed [kn]	Total Fuel [t]	Total NO_X [kg]	Total SO_2 [kg]	Total PM_{10} [kg]	Total CO_2 [t]
Route 00					
18	98.16	6805.2	4142.4	590.7	301.5
24	131.09	9415.2	5786.5	817.3	406.3
Route O1					
18	98.00	6791.0	4167.0	589.5	301.0
24	128.10	9167.6	5580.3	795.8	397.1
Route E1					
18	108.42	7516.8	4575.5	652.5	332.9
24	143.59	10 293.5	6386.7	893.6	444.9

scenarios are presented in Figs. 7 through 11, respectively. These figures depict the outcomes for the three studied routes at ship speeds of 18 and 24 knots. The concentration values of NO_x, SO_2 and PM_{10}, on the lowest model layer, averaged over the whole voyage duration, are shown in the shaded color palette (upper panel 18 knots, lower panel 24 knots), for all the routes (00, 01, and E1). The dots for the EWPs that delineate each route are colored as a function of the intensity of the computed meteo-dependent emission rate. The simulation results for the Calm and Heavy Weather scenario are reported from Figs. 7 to 8 and from Figs. 10 to 11, respectively.

The effects of the strong dependence of all the resistance components on ship speed reflect in the corresponding increase of the fuel consumption and emissions rates in passing from the speed value of 18 knots to 24 knots. As a consequence, comparing results with the same metocean conditions, lower concentrations emerge systematically from lower speed voyages, despite a greater voyage duration. Moreover, it must be noticed that different polluting impact patterns emerge from different routes and in particular, the impact on land areas is dependent on the route distance from the coast. The polluting impact variations due to the studied route variations are however lower than those due to ship speed variations. Despite calm weather ship emissions are lower, under the corresponding high pressure pattern the insuing vertical stratification and low wind conditions inhibit vertical and horizontal mixing with the result of a stronger tendency of pollutants to stagnate along the route. Only in the Southern part of the voyage, relatively stronger winds tend to advect and dilute the pollutants more effectively. In heavy weather conditions, though we have an increase of about 12–18% of emissions, these are more rapidly advected, reaching further areas, and more effectively diluted, also in relation to a more intense vertical overturning. The computed PM_{10} concentrations are those of the "primary" component, and they result to be lower and more localized along the route w.r.t. those of NO_x and SO_2, which result to be more widely dispersed and with higher values, more widely penetrating also on land. In real conditions, the penetrations of such pollutants on land can contribute to the chemical processes responsible for the generation of the "secondary" component of PM_{10}, e.g., see the works of the recent project SCIPPER (Majamäki et al., 2021). In Tables 4 and 5 it can be noticed that the total amount of emitted PM_{10} is an order of magnitude lower than the total amounts of NO_x and SO_2, accordingly the PM_{10} concentrations reported in the spatial maps are much lower than the concentrations of the other pollutants. It must be pointed out that concentration values of pollutants from a single ship, as in Figs. 7–11, are very low if compared with public safety regulation thresholds. Obviously, the overall impact of shipping activities comes from the superposition of the many contributions of all the ships in a given area. In a general scenario, such a superposition must be modeled accounting for the many non-linearities coming out from the combined complexity of meteo-marine dynamics and chemical behavior of the many involved compounds. As a consequence, the operational implementation of reliable modeling approaches requires sound preliminary scientific investigations and rigorous comparisons with reliable observed data. The work described here represents only a first step along this way.

6. Conclusions

In the present manuscript, the results of the development and first test of a comprehensive integrated framework for ship pollutant emissions and dispersion modeling have been presented. Its main functionalities are demonstrated and illustrated by considering NO_x, SO_2, PM_{10} and CO_2 emissions and by analyzing a specific case study Ro-Ro ship, involving scenario simulations in calm and heavy weather conditions. It is shown that the various components of the system allow

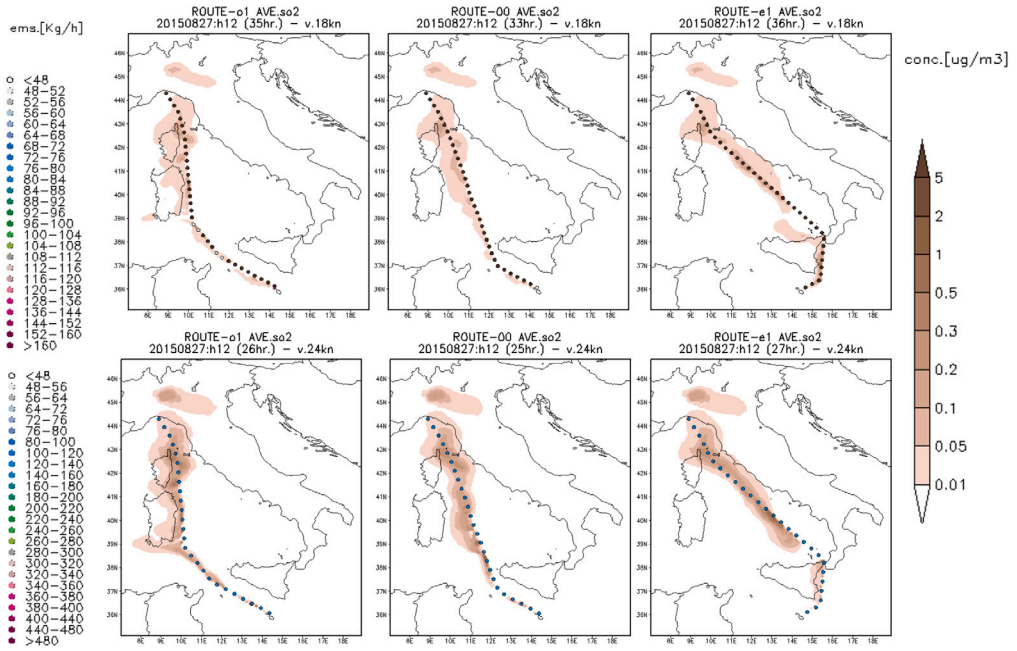

Fig. 8. Calm Weather: average values of computed of SO_2 concentration.

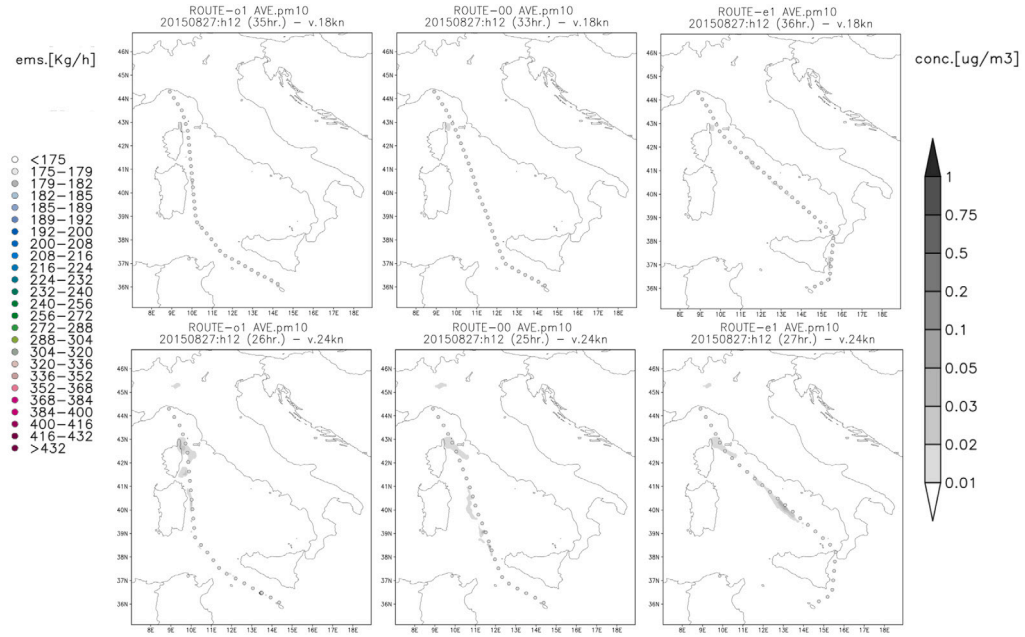

Fig. 9. Calm Weather: average values of computed of PM_{10} concentration.

for the investigation of the dynamics of ship pollutant emissions at different levels. Through the first modeling stages of the integrated system, the strong dependence of ship fuel consumption and emissions on ship speed clearly emerges, as well as the dependence on route length. Moreover, the comparison of the results obtained in calm metocean conditions, to be considered as the baseline situation, and in heavy weather allows appreciation of the relevant effects of the metocean conditions on increasing consumption, emission rates, and total quantities of the main pollutants. The interrelation between the specific route kinematics of the ship and the encountered metocean conditions emerges by comparing the results obtained along different routes and at different speeds. In the heavy weather scenario, thanks to relatively less intense metocean conditions, a longer route (route O1) resulted in being characterized by similar/slightly lower consumption and emissions than the more direct and shorter one (route 00). Through the last modeling stage, the complex and metocean-dependent mechanisms of pollutant dispersion can be accounted for. This allowed putting in evidence that the same heavy weather conditions that determine higher emissions are, at the same time, responsible for a stronger mixing producing lower surface pollutant concentration values with respect to calm weather conditions, despite lower emissions rates and totals in these latter situations. Moreover, this last part allows putting in evidence the coastal areas more impacted by the pollutants emitted by the ship at sea during the voyage, clearly showing the diverse roles in this of the different routes, of the voyage kinematics, and of the changing environmental conditions. The described results show the

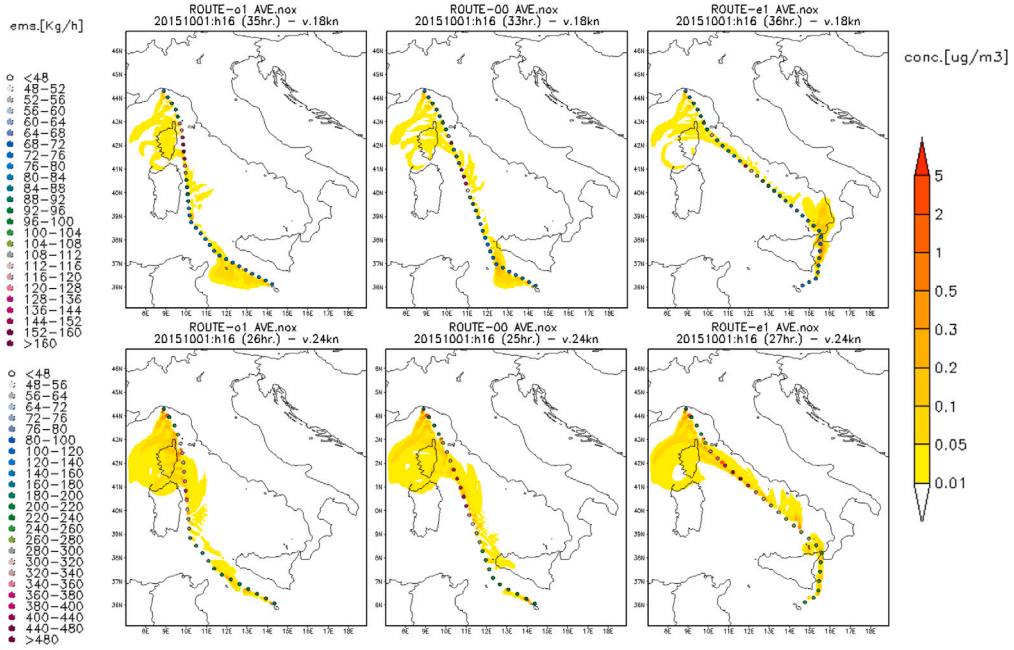

Fig. 10. Heavy Weather: average values of computed of NO_x concentration.

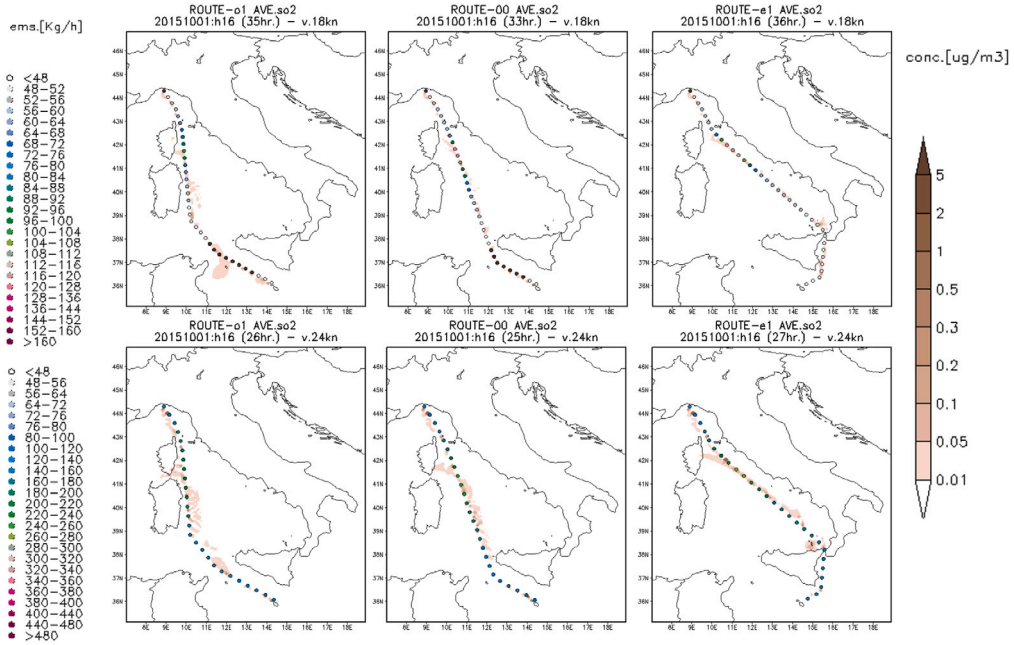

Fig. 11. Heavy Weather: average values of computed of SO_2 concentration.

capabilities of such a system to describe the detailed dynamics related to the pollutant emissions from ships, the effects of the kinematic and metocean conditions on the emission rates and on the fate of pollutants along and in the surroundings of ship routes. The integrated modeling system has the potential to allow very detailed impact studies focused on single voyages, or extended to a (not huge) population of ships, accounting for various critical features with a high level of detail and allowing a wide spectrum of investigations. As an example, in analyzing air quality conditions in port areas, the metocean and pollution modeling components could allow studying not trivial effects as those related to local breezes and to the complex dynamics of mixed layer thickens variations at the land–sea interface. As a further example, the interrelated ship modeling components, could allow investigating the different pollution regimes connected with the adoption of different fuel types, or the pollution reduction potentialities of cold-ironing. Moreover, the application of this system in the field of emission inventories construction could allow focusing on the relevant clues to be implemented in the simplified models in order to render them able to account for metocean conditions and also in simulations on extensive ship populations, as needed in such a field. A further level of investigation that will be afforded in the future is an extensive and systematic validation campaign, which although is not simple (Orović et al., 2022), will be a precious component of the final implementation

of a really reliable system. The results of these studies could be a precious resource at the decisional and planning levels for private shipping companies (optimization, monitoring and reducing impacts, planning and extending activities in an environmentally friendly manner) and for public institutions (monitoring, regulation, and investigation). The main elements that emerged from this first analysis suggest that, in its complete version, the system could find relevant applications in studies for the evaluation of the pollution impacts of marine navigation, in fleet management, and in the context of single ship operational optimization and weather routing.

CRediT authorship contribution statement

Andrea Orlandi: Conceptualization, Data curation, Formal analysis, Investigation, Methodology, Software, Validation, Visualization, Writing – original draft, Writing – review & editing. **Francesca Calastrini:** Conceptualization, Data curation, Formal analysis, Investigation, Methodology, Validation, Visualization, Writing – original draft, Writing – review & editing. **Miltiadis Kalikatzarakis:** Formal analysis, Methodology, Validation, Visualization, Writing – original draft. **Francesca Guarnieri:** Data curation, Investigation, Visualization. **Caterina Busillo:** Data curation, Investigation. **Andrea Coraddu:** Conceptualization, Data curation, Formal analysis, Investigation, Methodology, Supervision, Validation, Visualization, Writing – original draft, Writing – review & editing.

Declaration of competing interest

The authors declare that they have no known competing financial interests or personal relationships that could have appeared to influence the work reported in this paper.

Data availability

Data will be made available on request.

References

Abarbanel, H., 2013. Predicting the Future: Completing Models of Observed Complex Systems. Springer.

Abdelwahab, H., Wang, S., Parunov, J., Guedes Soares, C., 2023. A new model uncertainty measure of wave-induced motions and loads on a container ship with forward speed. J. Mar. Sci. Eng. 11.

Agreement, P., 2015. Paris agreement. In: Report of the Conference of the Parties to the United Nations Framework Convention on Climate Change (21st Session, 2015: Paris). Retrived December. Vol. 4, HeinOnline, p. 2017.

Alexandrov, V., Owczarz, W., Thomson, P., Zlatev, Z., 2004. Parallel runs of a large air pollution model on a grid of sun computers. Math. Comput. Simulation 65 (6), 557–577.

Ardhuin, F., 2021. Ocean Waves in Geosciences. Laboratoire d'Oceanographie Physique et Spatiale, Brest, France, http://dx.doi.org/10.13140/RG.2.2.16019.78888/5.

Asad, U., Tjong, J., Zheng, M., 2014. Exhaust gas recirculation – Zero dimensional modelling and characterization for transient diesel combustion control. Energy Convers. Manage. 86, 309–324.

Asariotis, R., Benamara, H., Finkenbrink, H., Hoffmann, J., Lavelle, J., Misovicova, M., Valentine, V., Youssef, F., 2019. Review of maritime transport. Tech. Rep., United Nations Conference on Trade and Development.

Baldi, F., Coraddu, A., 2022. Appendix B - Towards halving shipping GHG emissions by 2050: the IMO introduces the CII and the EEXI. In: Baldi, F., Coraddu, A., Mondejar, M.E. (Eds.), Sustainable Energy Systems on Ships. Elsevier, pp. 513–517.

Baldi, F., Johnson, H., Gabrielii, C., Andersson, K., 2014. Energy and exergy analysis of ship energy systems-the case study of a chemical tanker. In: 27th ECOS, International Conference on Efficiency, Cost, Optimization, Simulation and Environmental Impact of Energy Systems.

Baldi, F., Theotokatos, G., Andersson, K., 2015. Development of a combined mean value–zero dimensional model and application for a large marine four-stroke Diesel engine simulation. Appl. Energy 154, 402–415.

Balsamo, G., Engelen, R., Thiemert, D., Agusti-Panareda, A., Bousserez, N., Broquet, G., Brunner, D., Buchwitz, M., Chevallier, F., Choulga, M., et al., 2021. The CO2 human emissions (CHE) project: First steps towards a European operational capacity to monitor anthropogenic CO2 emissions. Front. Remote Sens. 2, 707247.

Becagli, S., Anello, F., Bommarito, C., Cassola, F., Calzolai, G., Di Iorio, T., di Sarra, A., Gómez-Amo, J., Lucarelli, F., Marconi, M., Meloni, D., Monteleone, F., Nava, S., Pace, G., Sferlazzo, D.M., Traversi, R., Udisti, R., 2017. Constraining the ship contribution to the aerosol of the central Mediterranean. Atmos. Chem. Phys. 17.

Becagli, S., Sferlazzo, D.M., Pace, G., di Sarra, A., Bommarito, C., Calzolai, G., Ghedini, C., Lucarelli, F., Meloni, D., Monteleone, F., Severi, M., Traversi, R., Udisti, R., 2012. Evidence for heavy fuel oil combustion aerosols from chemical analyses at the island of lampedusa: a possible large role of ships emissions in the Mediterranean. Atmos. Chem. Phys. 12.

Bejan, A., Gunes, A., Sahin, B., 2019. The evolution of air and maritime transport. Appl. Phys. Rev. 6.

Bertram, V., 2011. Practical Ship Hydrodynamics. Elsevier.

Bertram, V., Veelo, B., Soding, H., 2021. Program PDSTRIP: public domain strip method. software documentation.

Birk, L., 2019. Fundamentals of Ship Hydrodynamics: Fluid Mechanics, Ship Resistance and Propulsion. John Wiley & Sons.

Blendermann, W., 2013. Practical Ship and Offshore Structure Aerodynamics. Technische Universität Hamburg-Harburg.

Bonavita, M., Arcucci, R., Carrassi, A., Dueben, P., Geer, A., Le Saux, B., Longépé, N., Mathieu, P., Raynaud, L., 2021. Machine learning for earth system observation and prediction. Bull. Am. Meteorol. Soc. 102 (4), E710–E716.

Bousserez, N., 2019. Towards a prototype global CO2 emissions monitoring system for copernicus. arXiv:1910.11727.

Buhaug, Ø., Corbett, J.J., Endresen, Ø., Eyring, V., Faber, J., Hanayama, S., Lee, D.S., Lee, D., Lindstad, H., Markowska, A.Z., et al., 2009. Second Imo Ghg Study 2009. 20, International Maritime Organization (IMO) London, UK.

Buizza, C., Casas, C., Nadler, P., Mack, J., Marrone, S., Titus, Z., Le Cornec, C., Heylen, E., Dur, T., Ruiz, L., 2022. Data learning: Integrating data assimilation and machine learning. J. Comput. Sci. 58, 101525.

Bulian, G., Orlandi, A., 2022. Effect of environmental data uncertainty in the framework of second generation intact stability criteria. Ocean Eng. 253.

Calleya, J., Pawling, R., Greig, A., 2015. Ship impact model for technical assessment and selection of Carbon dioxide Reducing Technologies (CRTs). Ocean Eng. 97, 82–89.

Carlton, J., 2018. Marine Propellers and Propulsion. Butterworth-Heinemann.

Casey, M., Robinson, C., 2013. A method to estimate the performance map of a centrifugal compressor stage. J. Turbomach. 135 (2).

Catania, A., Finesso, R., Spessa, E., 2011. Predictive zero-dimensional combustion model for DI diesel engine feed-forward control. Energy Convers. Manage. 52 (10), 3159–3175.

Cavaleri, L., Alves, J.-H., Ardhuin, F., Babanin, A., Banner, M., Belibassakis, K., Benoit, M., Donelan, M., Groeneweg, J., Herbers, T., et al., 2007. Wave modelling–the state of the art. Prog. Oceanogr. 75 (4), 603–674.

Cimorelli, A., Perry, S., Venkatram, A., Weil, J., Paine, R., Wilson, R., Lee, R., Peters, W., Brode, R., 2005. AERMOD: A dispersion model for industrial source applications. Part I: General model formulation and boundary layer characterization. J. Appl. Meteorol. 44 (5), 682–693.

Coiffier, J., 2011. Fundamentals of Numerical Weather Prediction. Cambridge University Press.

Collett, R., Oduyemi, K., 1997. Air quality modelling: a technical review of mathematical approaches. Meteorol. Appl.: J. Forecasting, Practical Appl., Training Tech. Model. 4 (3), 235–246.

Conrad, R.E., 2005. SMP95: Standard ship motion program user manual. Tech. Rep., Naval Surface Warfare Center Carderock Division, Ship Hydromechanics Dept..

Cooper, D., Gustafsson, T., 2004. Methodology for calculating emissions from ships: 1. Update of emission factors. Tech. Rep., Report series for SMED and SMED&SLU, Nr 4, SMHI Swedish Meteorological and Hydrological Institute.

Coraddu, A., Figari, M., Savio, S., 2014. Numerical investigation on ship energy efficiency by Monte Carlo simulation. Proc. Inst. Mech. Eng. M 228 (3), 220–234.

Coraddu, A., Gaggero, S., Villa, D., Figari, M., 2012. A new approach in engine-propeller matching. In: 14th International Congress of the International Maritime Association of the Mediterranean, IMAM 2011. pp. 631–637.

Coraddu, A., Kalikatzarakis, M., Geertsma, R., Oneto, L., 2021a. Hybrid modelling approach of a four-stroke medium speed diesel engine. In: Proceedings of the 13th Symposium on High-Performance Marine Vehicles, HIPER'21. Technische Universität Hamburg-Harburg.

Coraddu, A., Kalikatzarakis, M., Oneto, L., Meijn, G., Godjevac, M., Geertsma, R., 2018. Ship diesel engine performance modelling with combined physical and machine learning approach. In: Proceedings of the International Ship Control Systems Symposium (ISCSS). Vol. 2, p. 4.

Coraddu, A., Kalikatzarakis, M., Theotokatos, G., Geertsma, R., Oneto, L., 2021b. Physical and data-driven models hybridisation for modelling the dynamic state of a four-stroke marine diesel engine. In: Engine Modeling and Simulation. Springer, pp. 145–193.

Coraddu, A., Oneto, L., Baldi, F., Anguita, D., 2017. Vessels fuel consumption forecast and trim optimisation: a data analytics perspective. Ocean Eng. 130, 351–370.

Corbett, J., Winebrake, J., Carr, E., Jalkanen, J., Johansson, L., Prank, M., Sofiev, M., 2016. Study on effects of the entry into force of the global 0.5% fuel oil sulphur content limit on human health. Tech. Rep.; 70/INF.34, IMO/MEPC.

Council, N.R., 2012. Assessing the reliability of complex models: Mathematical and statistical foundations of verification, validation, and uncertainty quantification. Tech. Rep., The National Academies Press, Washington, DC.
Crisp, D., van der Gon, H., Engelen, R., Janssens-Maenhout, G., Heimann, M., Rayner, P., Scholze, M., 2015. Towards a European operational observing system to monitor fossil CO2 emissions. Final report from the expert group. Tech. Rep., EU, Directorate-General for Internal Market, Industry, Entrepreneurship and SMEs, Directorate I — Space Policy, Copernicus and Defence, Unit I.2 — Copernicus.
Dabdub, D., Seinfeld, J., 1996. Parallel computation in atmospheric chemical modeling. Parallel Comput. 22 (1), 111–130.
Dern, J., Quenez, J., Wilson, P., 2016. Compendium of Ship Hydrodynamics. Les presses de l'ENSTA.
Di Natale, F., Carotenuto, C., 2015. Particulate matter in marine diesel engines exhausts: Emissions and control strategies. Transp. Res. D 40, 166–191.
Diesch, J.-M., Drewnick, F., Klimach, T., Borrmann, S., 2013. Investigation of gaseous and particulate emissions from various marine vessel types measured on the banks of the Elbe in Northern Germany. Atmos. Chem. Phys. 13 (7), 3603–3618.
Ding, Y., Stapersma, D., Knoll, H., Grimmelius, H., Netherland, T., 2010. Characterising heat release in a diesel engine: A comparison between seiliger process and vibe model. In: CIMAC International Council on Combustion engines. pp. 1–13.
Draxler, R., Hess, G., 1998. An overview of the HYSPLIT_4 modelling system for trajectories. Aust. Meteorol. Mag. 47 (4), 295–308.
el Moctar, B., Schellin, T., Söding, H., 2021. Numerical Methods for Seakeeping Problems. Springer.
Faltinsen, O., 1993. Sea Loads on Ships and Offshore Structures. Vol. 1, Cambridge University Press.
Finesso, R., Spessa, E., 2014. A real time zero-dimensional diagnostic model for the calculation of in-cylinder temperatures, HRR and nitrogen oxides in diesel engines. Energy Convers. Manage. 79, 498–510.
Fu, M., Liu, H., Jin, X., He, K., 2017. National- to port-level inventories of shipping emissions in China. Environ. Res. Lett. 12.
Gabrielli, G., von Karman, T., 1950. What price of speed? Mech. Eng. 72.
Garcia-Menendez, F., Odman, M., 2011. Adaptive grid use in air quality modeling. Atmosphere 2 (3), 484–509.
Geertsma, R., Negenborn, R., Visser, K., Loonstijn, M., Hopman, J., 2017. Pitch control for ships with diesel mechanical and hybrid propulsion: Modelling, validation and performance quantification. Appl. Energy 206, 1609–1631.
Gourlay, T., von Graefe, A., Shigunov, V., Lataire, E., 2015. Comparison of aqwa, gl rankine, moses, octopus, pdstrip and wamit with model test results for cargo ship wave-induced motions in shallow water. In: International Conference on Offshore Mechanics and Arctic Engineering. Vol. 56598, American Society of Mechanical Engineers, V011T12A006.
Grigoropoulos, G., Harries, S., Damala, D.P., Heimann, J., 2003. Seakeeping assessment for high-speed monohulls – a comparative study. In: 8th Intl. Marine Design Conference IMDC'03, Athens, Greece.
Grimmelius, H., 2003. Simulation models in marine engineering: from training to concept exploration. In: 2nd International EuroConference on Computer and IT Applications in the Maritime Industries. pp. 502–515.
Grimmelius, H., Boonen, E., Nicolai, H., Stapersma, D., 2010. The integration of mean value first principle diesel engine models in dynamic waste heat and cooling load analysis. In: CIMAC Congress, Bergen, Norway. Vol. 31, p. 51.
Guachamin-Acero, W., Portilla, J., 2022. Prediction of dynamic responses for execution of marine operations using partitioning of multimodal directional wave spectra and machine learning regression models. Ocean Eng. 262, 112157.
Guan, C., Theotokatos, G., Zhou, P., Chen, H., 2014. Computational investigation of a large containership propulsion engine operation at slow steaming conditions. Appl. Energy 130, 370–383.
Guedes Soares, C., 1991. Effect of transfer function uncertainty on short-term ship response. Ocean Eng. 18 (4).
Hanson, R., Salimian, S., 1984. Survey of rate constants in the N/H/O system. In: Combustion Chemistry. Springer, pp. 361–421.
He, L., Wang, J., Liu, Y., Zhang, Y., He, C., Yu, Q., Ma, W., 2021. Selection of onshore sites based on monitoring possibility evaluation of exhausts from individual ships for Yantian Port, China. Atmos. Environ. 247, 118187.
Heywood, J., 1988. Internal Combustion Engines Fundamentals, 1988 Ch. 11. McGraw-Hill, New York.
Holmes, N., Morawska, L., 2006. A review of dispersion modelling and its application to the dispersion of particles: an overview of different dispersion models available. Atmos. Environ. 40 (30), 5902–5928.
Houghton, I.A., Hegermiller, C., Teicheira, C., Smit, P., 2022. Operational assimilation of spectral wave data from the sofar spotter network. Geophys. Res. Lett..
Huszar, P., Cariolle, D., Paoli, R., Halenka, T., Belda, M., Schlager, H., Miksovsky, J., Pisoft, P., 2010. Modeling the regional impact of ship emissions on NO x and ozone levels over the Eastern Atlantic and Western Europe using ship plume parameterization. Atmos. Chem. Phys. 10 (14), 6645–6660.
IMO, 2011. Amendments to the annex of the protocol of 1997 to amend the international convention for the prevention of pollutiong from ships, 1973, as modified by the protocol of 1978 relating thereto (Inclusion of regulations on energy efficiency for ships in MARPOL Annex VI). URL https://www.imo.org/en/OurWork/Environment/Pages/Technical-and-Operational-Measures.aspx.
International Standards Organization, 2015. Guidelines for the assessment of speed and power performance by analysis of speed trial data.
Jalkanen, J., Brink, A., Kalli, J., Pettersson, H., Kukkonen, J., Stipa, T., 2009. A modelling system for the exhaust emissions of marine traffic and its application in the Baltic Sea area. Atmos. Chem. Phys. 9.
Jalkanen, J., Johansson, L., Kukkonen, 2016. A comprehensive inventory of ship traffic exhaust emissions in the European sea areas in 2011. Atmos. Chem. Phys. 16.
Janssens-Maenhout, G., Pinty, B., Dowell, M., Zunker, H., Andersson, E., Balsamo, G., Bézy, J.-L., Brunhes, T., Bösch, H., Bojkov, B., et al., 2020. Toward an operational anthropogenic CO 2 emissions monitoring and verification support capacity. Bull. Am. Meteorol. Soc. 101 (8), E1439–E1451.
Journée, J., Meijers, J., 1980. Ship Routeing for Optimum Performance. Delft University of Technology.
Kalikatzarakis, M., Coraddu, A., Theotokatos, G., Oneto, L., 2021. Development of a zero-dimensional model and application on a medium-speed marine four-stoke diesel engine. In: 3rd International Conference on Modelling and Optimisation of Ship Energy Systems.
Kalnay, E., 2003. Atmospheric Modeling, Data Assimilation and Predictability. Cambridge University Press.
Kämpf, J., 2010. Advanced Ocean Modelling: Using Open-Source Software. Springer Science & Business Media.
Kim, S., 2011. CFD as a seakeeping tool for ship design. Int. J. Nav. Archit. Ocean Eng. 3 (1), 65–71.
Kim, J., Kim, K., Kim, Y., Van, S., Kim, H., 2011. Comparison of potential and viscous methods for the nonlinear ship wave problem. Int. J. Nav. Archit. Ocean Eng. 3 (3), 159–173.
Kim, S., Roh, M., Oh, M., Park, S., Kim, I., 2020. Estimation of ship operational efficiency from AIS data using big data technology. Int. J. Nav. Archit. Ocean Eng. 12, 440–454.
Komen, G., Cavaleri, L., Donelan, M., Hasselmann, K., Hasselmann, S., Janssen, P., 1994. Dynamics and Modelling of Ocean Waves. Cambridge University Press.
Lee, J., Nam, Y., Kim, Y., Liu, Y., Lee, J., Yang, H., 2022. Real-time digital twin for ship operation in waves. Ocean Eng. 266, 112867.
Leelőssy, A., Lagzi, I., Kovács, A., Mészáros, R., 2018. A review of numerical models to predict the atmospheric dispersion of radionuclides. J. Environ. Radioact. 182, 20–33.
Lefèvre, J.-M., Aouf, L., 2012. Latest developments in wave data assimilation. In: Workshop on Ocean Waves. ECMWF.
Lewis, E.V., 1988. Principles of naval architecture second revision. Jersey: Sname 2.
Ličer, M., Smerkol, P., Fettich, A., Ravdas, M., Papapostolou, A., Mantziafou, A., Strajnar, B., Cedilnik, J., Jeromel, M., Jerman, J., 2016. Modeling the ocean and atmosphere during an extreme bora event in northern Adriatic using one-way and two-way atmosphere–ocean coupling. Ocean Sci. 12 (1), 71–86.
Liu, Z., Zuo, Q., Wu, G., Li, Y., 2018. An artificial neural network developed for predicting of performance and emissions of a spark ignition engine fueled with butanol-gasoline blends. Adv. Mech. Eng. 10 (1), 1687814017748438.
Livanos, G., Papalambrou, G., Kyrtatos, N., Christou, A., 2007. Electronic engine control for ice operation of tankers. In: Proceedings of the 25th CIMAC World Congress on Combustion Engine Technology, Vienna, Austria. pp. 21–24.
Lu, R., Turan, O., Boulougouris, E., Banks, C., Incecik, A., 2015. A semi-empirical ship operational performance prediction model for voyage optimization towards energy efficient shipping. Ocean Eng. 110, 18–28.
Majamäki, E., Jalkanen, J.-P., Matthias, V., Fridell, E., 2021. Deliverable D4.2. Updated inventories on regional shipping activity and port regions. Tech. Rep., E.U. H2020, SCIPPER Project, No. 814893, https://www.scipper-project.eu/.
Malkhede, D.N., Seth, B., Dhariwal, H., 2005. Mean value model and control of a marine turbocharged diesel engine. Tech. Rep., SAE Technical Paper.
Maroteaux, F., Saad, C., 2015. Combined mean value engine model and crank angle resolved in-cylinder modeling with NOx emissions model for real-time Diesel engine simulations at high engine speed. Energy 88, 515–527.
Matulja, D., Sportelli, M., Prpić-Oršić, J., Guedes Soares, C., 2010. Methods for estimation of ships added resistance in regular waves. In: The 19th Symposium on Theory and Practice of Shipbuilding Sorta.
Merker, G., Schwarz, C., Stiesch, G., Otto, F., 2005. Simulating Combustion: Simulation of Combustion and Pollutant Formation for Engine Development. Springer Science & Business Media.
Miller, R., 2007. Numerical Modeling of Ocean Circulation. Cambridge University Press.
Mittendorf, M., Nielsen, U.D., Bingham, H., Liu, S., 2022. Towards the uncertainty quantification of semi-empirical formulas applied to the added resistance of ships in waves of arbitrary heading. Ocean Eng. 251.
Mohammadkhani, F., Yari, M., Ranjbar, F., 2019. A zero-dimensional model for simulation of a Diesel engine and exergoeconomic analysis of waste heat recovery from its exhaust and coolant employing a high-temperature Kalina cycle. Energy Convers. Manage. 198, 111782.
Molnar Jr., F., Szakaly, T., Meszaros, R., Lagzi, I., 2010. Air pollution modelling using a graphics processing unit with CUDA. Comput. Phys. Comm. 181 (1), 105–112.
Moore, A.M., Martin, M.J., Akella, S., Arango, H.G., Balmaseda, M., Bertino, L., Ciavatta, S., Cornuelle, B., Cummings, J., Frolov, S., Lermusiaux, P., Oddo, P., Oke, P.R., Storto, A., Teruzzi, A., Vidard, A., Weaver, A.T., 2019. Synthesis of ocean observations using data assimilation for operational, real-time and reanalysis systems: A more complete picture of the state of the ocean. Front. Mar. Sci. 6 (90).

Murena, F., Mocerino, L., Quaranta, F., Toscano, D., 2018. Impact on air quality of cruise ship emissions in Naples, Italy. Atmos. Environ. 187, 70–83.
Neroda, A., Mishukov, V., Goryachev, V., Simonenkov, D., Goncharova, A., 2014. Radioactive isotopes in atmospheric aerosols over Russia and the Sea of Japan following nuclear accident at Fukushima Nr. 1 Daiichi Nuclear Power Station in March 2011. Environ. Sci. Pollut. Res. 21 (8), 5669–5677.
Nielsen, U., Jensen, J., 2011. A novel approach for navigational guidance of ships using onboard monitoring systems. Ocean Eng. 38 (2–3), 444–455.
Nikzadfar, K., Shamekhi, A.H., 2014. Investigating the relative contribution of operational parameters on performance and emissions of a common-rail diesel engine using neural network. Fuel 125, 116–128.
Nikzadfar, K., Shamekhi, A., 2015. An extended mean value model (EMVM) for control-oriented modeling of diesel engines transient performance and emissions. Fuel 154, 275–292.
Nunes, R., Alvim-Ferraz, M., Martins, F., Sousa, S., 2017. The activity-based methodology to assess ship emissions-A review. Environ. Pollut. 231, 87–103.
Ogilvie, T.F., Tuck, E.O., 1969. A rational strip theory of ship motions: part I. Tech. Rep., University of Michigan.
Oikonomakis, A., Galeazzi, R., Dietz, J., Nielsen, U., Holst, K., 2019. Application of sensor fusion to drive vessel performance. In: 4th Hull Performance & Insight Conference (HullPIC'19), Gubbio, Italy. pp. 6–8.
Orlandi, A., 2012. Integration of Meteo-Marine Forecast Data with Ship Seakeeping and Powering Computational Techniques (Ph.D. thesis). Ph.D. thesis in Naval Architecture and Marine Engineering, Supervisor: Dario Bruzzone.
Orlandi, A., Bruzzone, D., 2012. Numerical weather and wave prediction models for weather routing, operation planning and ship design: The relevance of multimodal wave spectra. In: Sustainable Maritime Transportation and Exploitation of Sea Resources. Taylor & Francis Group London, pp. 817–826.
Orlandi, A., Cappugi, A., Mari, R., Pasi, F., Ortolani, A., 2021. Meteorological navigation by integrating metocean forecast data and ship performance models into an ecdis-like e-navigation prototype interface. J. Mar. Sci. Eng. 9 (5), 502.
Orlandi, A., Cappugi, A., Mari, R., Pasi, F., Ortolani, A., 2022. Meteorological navigation by an ECDIS-like system: discussing the algorithms and demostrating the functionalities for conventional propulsion and for sail-assisted ships. In: 21st Conference on Computer and IT.
Orlandi, A., Pasi, F., Capecchi, V., Coraddu, A., Villa, D., 2015. Powering and seakeeping forecasting for energy efficiency: assessment of the fuel savings potential for weather routing by in-service data and ensemble prediction techniques. Towards Green Mar. Technol. Transp. 31.
Orović, J., Valčić, M., Knežević, V., Pavin, Z., 2022. Comparison of the on board measured and simulated exhaust gas emissions on the ro-pax vessels. Atmosphere 13 (5), 794.
Orych, M., Östberg, M., Kjellberg, M., Werner, S., Larsson, L., 2023. Speed and delivered power in waves—Predictions with CFD simulations at full scale. Ocean Eng. 285, 115289.
Özener, O., Yüksek, L., Özkan, M., 2013. Artificial neural network approach to predicting engine-out emissions and performance parameters of a turbo charged diesel engine. Therm. Sci. 17 (1), 153–166.
Pacheco, M., Guedes Soares, C., 2007. Ship weather routing based on seakeeping performance. Adv. Mar. Struct. 71–78.
Papanikolaou, A., 2019. A Holistic Approach to Ship Design. Springer.
Parisella, G., Gourlay, T., 2016. Comparison of Open-Source Code Nemoh with Wamit for Cargo Ship Motions in Shallow Water. 23, Centre for Marine Science and Technology, Curtin University.
Parunov, J., Guedes Soares, C., Hirdaris, S., Iijima, K., Wang, X., Brizzolara, S., Qiu, W., Mikuli, A., Wang, S., Abdelwahab, H., 2022. Benchmark study of global linear wave loads on a container ship with forward speed. Mar. Struct. 84.
Perera, L., Soares, C., 2017. Weather routing and safe ship handling in the future of shipping. Ocean Eng. 130, 684–695.
Pielke, R., 1984. Mesoscale Meteorological Modeling Academic Press. New York, NY, USA, pp. 1–612.
Pinardi, N., Cavaleri, L., Coppini, G., De Mey, P., Fratianni, C., Huthnance, J., Lermusiaux, P.F.J., Navarra, A., Preller, R., Tibaldi, S., 2017. From weather to ocean predictions: an historical viewpoint. J. Mar. Res. 75, 103–159.
Poplawski, K., Setton, E., McEwen, B., Hrebenyk, D., Graham, M., Keller, P., 2011. Impact of cruise ship emissions in Victoria, BC, Canada. Atmos. Environ. 45 (4), 824–833.
Pozorski, J., Minier, J., 1998. On the Lagrangian turbulent dispersion models based on the Langevin equation. Int. J. Multiph. Flow 24 (6), 913–945.
Price, W.G., 1974. Probabilistic theory of ship dynamics. University College London, Published by: Chapman & Hall Ltd, London, ISBN: 0 412 12430 0, Printed in the United Kingdom.
Rakopoulos, C., Hountalas, D., Tzanos, E., Taklis, G., 1994. A fast algorithm for calculating the composition of diesel combustion products using 11 species chemical equilibrium scheme. Adv. Eng. Softw. 19 (2), 109–119.
Reichel, M., Minchev, A., Larsen, N., 2014. Trim optimisation-theory and practice. TransNav: Int. J. Mar. Navig. Saf. Sea Transp. 8.
Rohsenow, W., Hartnett, J., 1988. Handbook of Heat Transfer Fundamentals, 2nd Edition. McGraw-Hill, New York.
Sapra, H., Godjevac, M., De Vos, P., Van Sluijs, W., Linden, Y., Visser, K., 2020. Hydrogen-natural gas combustion in a marine lean-burn SI engine: A comparitive analysis of Seiliger and double Wiebe function-based zero–dimensional modelling. Energy Convers. Manage. 207, 112494.
Saydam, A.Z., Taylan, M., 2018. Evaluation of wind loads on ships by CFD analysis. Ocean Eng. 158, 54–63.
Schneider, R., Bonavita, M., Geer, A., Arcucci, R., Dueben, P., Vitolo, C., Le Saux1, B., Demir, B., Mathieuet, P., 2022. ESA-ECMWF Report on recent progress and research directions in machine learning for Earth System observation and prediction. npj Clim. Atmos. Sci. 5 (51), 1–5.
Scire, J., Strimaitis, D., Yamartino, R., et al., 2000a. A user's guide for the CALMET meteorological model. Earth Tech, USA 37.
Scire, J., Strimaitis, D., Yamartino, R., et al., 2000b. A user's guide for the CALPUFF dispersion model. Earth Tech, Inc 521, 1–521.
Segersson, D., 2013. A dynamic model for shipping emissions Adaptation of Airviro and application in the Baltic Sea. Tech. Rep., SMHI, METEOROLOGY, 153, SMHI.
Shin, S., Lee, Y., Kim, M., Park, J., Lee, S., Min, K., 2020. Deep neural network model with Bayesian hyperparameter optimization for prediction of NOx at transient conditions in a diesel engine. Eng. Appl. Artif. Intell. 94, 103761.
Simonsen, M., Larsson, E., Mao, W., Ringsberg, J., 2015. State-of-the-art within ship weather routing. In: International Conference on Offshore Mechanics and Arctic Engineering. Vol. 56499, American Society of Mechanical Engineers, V003T02A053.
Smith, T., Jalkanen, J., Anderson, B., Corbett, J., Faber, J., Hanayama, S., O'keeffe, E., Parker, S., Johansson, L., Aldous, L., et al., 2014. Third imo ghg study 2014. Tech. Rep., International Maritime Organization (IMO), London.
Spentza, E., Besio, G., Mazzino, A., Gaggero, T., Villa, D., 2017. A ship weather-routing tool for route evaluation and selection: influence of the wave spectrum. In: International Congress of the International Maritime Association of the Mediterranean (IMAM 2017). pp. 453–462.
Stockie, J.M., 2011. The mathematics of atmospheric dispersion modeling. Siam Rev. 53 (2), 349–372.
Stoumpos, S., Theotokatos, G., Boulougouris, E., Vassalos, D., Lazakis, I., Livanos, G., 2018. Marine dual fuel engine modelling and parametric investigation of engine settings effect on performance-emissions trade-offs. Ocean Eng. 157, 376–386.
Stoumpos, S., Theotokatos, G., Mavrelos, C., Boulougouris, E., 2020. Towards marine dual fuel engines digital twins-integrated modelling of thermodynamic processes and control system functions. J. Mar. Sci. Eng. 8 (3), 200.
Syed, J., Baig, R.U., Algarni, S., Murthy, S., Masood, M., Inamurrahman, M., 2017. Artificial neural network modeling of a hydrogen dual fueled diesel engine characteristics: An experiment approach. Int. J. Hydrogen Energy 42 (21), 14750–14774.
Takami, T., Nielsen, U., Jensen, J., 2021. Real-time deterministic prediction of wave-induced ship responses based on short-time measurements. Ocean Eng. 221, 108503.
Tang, L., Ramacher, M., Moldanová, J., Matthias, V., Karl, M., Johansson, L., Jalkanen, J., Yaramenka, K., Aulinger, A., Gustafsson, M., 2020. The impact of ship emissions on air quality and human health in the Gothenburg area–Part 1: 2012 emissions. Atmos. Chem. Phys. 20 (12), 7509–7530.
Tang, Y., Zhang, J., Gan, H., Jia, B., Xia, Y., 2017. Development of a real-time two-stroke marine diesel engine model with in-cylinder pressure prediction capability. Appl. Energy 194, 55–70.
Taskar, B., Andersen, P., 2021. Comparison of added resistance methods using digital twin and full-scale data. Ocean Eng. 229, 108710.
Tay, Z., Hadi, J., Chow, F., Loh, D., Konovessis, D., 2021. Big data analytics and machine learning of harbour craft vessels to achieve fuel efficiency: a review. J. Mar. Sci. Eng. 9 (12), 1351.
Tezdogan, T., Demirel, Y., Kellett, P., Khorasanchi, M., Incecik, A., Turan, O., 2015. Full-scale unsteady RANS CFD simulations of ship behaviour and performance in head seas due to slow steaming. Ocean Eng. 97, 186–206.
Theotokatos, G., 2008. Ship propulsion plant transient response investigation using a mean value engine model. Int. J. Energy 2 (4), 66–74.
Theotokatos, G., 2010. On the cycle mean value modelling of a large two-stroke marine diesel engine. Proc. Inst. Mech. Eng. M 224 (3), 193–205.
Theotokatos, G., Guan, C., Chen, H., Lazakis, I., 2018. Development of an extended mean value engine model for predicting the marine two-stroke engine operation at varying settings. Energy 143, 533–545.
Thykier-Nielsen, S., Deme, S., Mikkelsen, T., 1999. Description of the atmospheric dispersion module RIMPUFF. Riso National Laboratory, PO Box 49.
Tolman, H.L., et al., 2009. User manual and system documentation of WAVEWATCH III TM version 3.14. Technical note, MMAB Contribution, 276, p. 220.
Toscano, D., Murena, F., Quaranta, F., Mocerino, L., 2021. Assessment of the impact of ship emissions on air quality based on a complete annual emission inventory using AIS data for the port of Naples. Ocean Eng. 232, 109166.
Townsin, L., Kwon, J., Baree, S., Kim, Y., 1993. Estimating the influence of weather on ship performance. RINA Trans. 135.
Trancossi, M., 2016. What price of speed? A critical revision through constructal optimization of transport modes. Int. J. Energy Environ. Eng. 7.
Trozzi, C., 2010. Emission estimate methodology for maritime navigation. Techne Consulting, Rome.
Trozzi, C., De Lauretis, R., 2019. Air pollutant emission inventory guidebook. Tech. Rep., EMEP/EEA.

Tsitsilonis, K., Theotokatos, G., Patil, C., Coraddu, A., 2023. Health assessment framework of marine engines enabled by digital twins. Int. J. Engine Res. 14680874221146835.

Tsujimoto, M., Orihara, H., 2019. Performance prediction of full-scale ship and analysis by means of on-board monitoring (Part 1 ship performance prediction in actual sea. J. Mar. Sci. Technol. 24.

Valcke, S., Balaji, V., Craig, A., DeLuca, C., Dunlap, R., Ford, R., Jacob, R., Larson, J., O'Kuinghttons, R., Riley, G., 2012. Coupling technologies for earth system modelling. Geosci. Model Dev. 5 (6), 1589–1596.

van Aardenne, J., Colette, A., Degraeuwe, B., Hammingh, P., De Vlieger, I., 2013. The impact of international shipping on European air quality and climate forcing. EEA Technical Report, 4.

van den Boom, H., Mennen, G., Verkuyl, J., 2006. Recommended practice for speed trials.

Veen, D., Gourlay, T., 2012. A combined strip theory and smoothed particle hydrodynamics approach for estimating slamming loads on a ship in head seas. Ocean Eng. 43, 64–71.

Vossen, C., Kleppe, R., Hjørungnes, S., 2013. Ship design and system integration. In: DMK Conference.

Wang, H., Gan, H., Theotokatos, G., 2020. Parametric investigation of pre-injection on the combustion, knocking and emissions behaviour of a large marine four-stroke dual-fuel engine. Fuel 281, 118744.

Wang, W., Wu, T., Zhao, D., Guo, C., Luo, W., Pang, Y., 2019. Experimental–numerical analysis of added resistance to container ships under presence of wind–wave loads. PLoS One 14 (8).

Wartsila, 2022. Wärtsilä smart voyage optimisation. URL www.wartsila.com/smart-voyage.

Watson, N., Janota, M., 1982. Turbocharging the Internal Combustion Engine. Macmillan International Higher Education.

Winnes, H., Fridell, E., 2009. Particle emissions from ships: dependence on fuel type. J. Air Waste Manag. Assoc. 59 (12), 1391–1398.

Woschni, G., 1967. A universally applicable equation for the instantaneous heat transfer coefficient in the internal combustion engine. Tech. Rep., SAE Technical paper.

Xiang, L., Theotokatos, G., Ding, Y., 2019. Investigation on gaseous fuels interchangeability with an extended zero-dimensional engine model. Energy Convers. Manage. 183, 500–514.

Yoon, H., Nguyen, V., Nguyen, T., 2017. Optimal weather routing considering seakeeping performance based on the model test. In: Marine Navigation. CRC Press, pp. 245–252.

Yum, K., Taskar, B., Pedersen, E., Steen, S., 2017. Simulation of a two-stroke diesel engine for propulsion in waves. Int. J. Nav. Archit. Ocean Eng. 9 (4), 351–372.

ZeroNorth, 2022. Whitepaper: Fuel consumption model accuracy standard. URL https://zeronorth.com/compass/fuel-consumption-accuracy-standard-white-paper.

Zhang, W., Moctar, O., Schellin, T., 2020. Numerical study on wave-induced motions and steady wave drift forces for ships in oblique waves. Ocean Eng. 196.

Zhang, Y., WeiWang, J., Peng, Y., Wu, X., Feng, X., 2017. Inland port vessel emissions inventory based on ship traffic emission assessment model–automatic identification system. Adv. Mech. Eng. 9.

Zhu, Y., Zuo, Y., Li, T., 2021. Modeling of ship fuel consumption based on multisource and heterogeneous data: Case study of passenger ship. J. Mar. Sci. Eng. 9 (3), 273.